

# The origin of massive O-type field stars<sup>\*,\*\*</sup>

## I. A search for clusters

W. J. de Wit<sup>1</sup>, L. Testi<sup>1</sup>, F. Palla<sup>1</sup>, L. Vanzini<sup>2</sup>, and H. Zinnecker<sup>3</sup>

<sup>1</sup> INAF - Osservatorio Astrofisico di Arcetri, Largo E. Fermi 5, 50125 Florence, Italy  
e-mail: dewit@arcetri.astro.it

<sup>2</sup> ESO, Alonso de Cordova 3107, Santiago, Chile

<sup>3</sup> Astrophysikalisches Institut Potsdam, An der Sternwarte 16, 14482 Potsdam, Germany

Received 16 March 2004 / Accepted 12 May 2004

**Abstract.** We present a study aimed at clarifying the birthplace for 43 massive O-type *field* stars. In this first paper we present the observational part: a search for stellar clusters near the target stars. We derive stellar density maps at two different resolving scales, viz.  $\sim 0.25$  pc and  $\sim 1.0$  pc from NTT and TNG imaging and the 2MASS catalogue. These scales are typical for cluster sizes. The main result is that the large majority of the O-type field population are isolated stars: only 12% (5 out of 43) of the O-type field stars is found to harbour a small-scale stellar cluster. We review the literature and aim at characterizing the stellar field of each O-type field star with the emphasis on star formation and the presence of known young stellar clusters. An analysis of the result of this paper and a discussion of the O-type field population as products of a dynamical ejection event is presented in an accompanying paper.

**Key words.** stars: early-type – stars: formation

## 1. Introduction

We present the first of two papers that treat the search for the origin of formation of massive O-type field stars in the Galaxy. The O-type field stars are isolated massive stars in the Galactic field and are not known to be members of stellar clusters and/or OB-associations. These stars constitute about 20% of the total number of O-type stars in the Galaxy (see e.g., Gies 1987; Mason et al. 1998). Their relative small number and generally large distances combined with an incomplete census of clusters/OB associations throughout the Galaxy have led people to speculate that the birthplace of the O-type field stars could well be a cluster environment. If confirmed, this would be an important finding in light of the ongoing discussion on the formation of a high mass star, be it by stellar coalescence (Bonnell et al. 1998, 2004) or conversely by mass accretion through a circumstellar disk/envelope (e.g., Yorke & Sonnhalter 2002).

In this first contribution of our study on O-type field stars, we present deep near infrared photometric observations to

search for clusters of low mass stars near the massive field stars. Practically we probe for stellar density enhancements with respect to the back/fore-ground stars on small ( $\sim 5$  pc) and large ( $\sim 20$  pc) scale. We complement the cluster search with a literature overview for each target star in our sample with the emphasis on the presence of nearby ( $< 65$  pc) young stellar clusters, associations or star forming regions. In this way we hope to elucidate the formation history of massive field stars. The discussion of the results of this study will be combined in an accompanying paper with the interpretation of the massive O-type field stars as the product of a dynamical ejection.

The organization of this paper is as follows. In Sect. 2 we discuss our working definition for field stars, the number of O-type stars in the field and the sample selection. In Sect. 3 the observations and the analysis method are described. Each O-type field star is reviewed and its stellar density maps presented in Sect. 4. We summarize the results in Sect. 5.

## 2. The number of O-type field stars

### 2.1. Definition of names

The definition of a field star is a negative one. Field stars are those objects that are not member of any known spatial concentration of stars, either a cluster or an association of stars (and membership can be established using different techniques).

\* Based on observations collected at the European Southern Observatory, Chile, and at the Italian Telescopio Nazionale Galileo (TNG) operated on the island of La Palma by the Centro Galileo Galilei of the CNAA (Consorzio Nazionale per l'Astronomia e l'Astrofisica) at the Spanish Observatorio del Roque de los Muchachos of the Instituto de Astrofisica de Canarias.

\*\* Table 2 and Figs. 4 to 17 are available in electronic form at <http://www.edpsciences.org>

**Table 1.** O star catalogues. In Col. 1 the name and reference of the catalogue, Col. 2 the total number of entries, Col. 3 all entries with an apparent visual magnitude less than  $8^m$ . In Col. 4 the subset and percentage of field stars with  $V < 8^m$ .

Name	$N_{\text{tot}}$	$N_{\text{tot}}(V < 8^m)$	$N_{\text{field}}(V < 8^m)$
COS82 <sup>1</sup>	765	205	91 (44%)
G87 <sup>2</sup>	195	195	43 (22%)
M98 <sup>3</sup>	227	193	39 (20%)
M04 <sup>4</sup>	370	185	35 (19%)

1. Garmany et al. (1982); 2. Gies (1987); 3. Mason et al. (1998);  
4. Maíz-Apellániz et al. (2004).

In general, field stars form the old population of a Galaxy and should therefore be of low mass.

However, there exists a number of stars among the field population that are known to be massive and therefore are much younger than the average age of the field. They come in two varieties. Historically, most attention was devoted to those massive field stars that are known to have (or have had) high spatial velocities, i.e. the runaway stars (see Blaauw 1961). From a stellar population point of view these stars are a subset of the field, however when deriving physical quantities of stellar clusters, runaways should be considered as cluster members.

The second group of massive stars that are located in the field are simply those O-type stars without large spatial velocities. They have received less attention in the literature as a group, since it is expected that they are unrecognized runaway stars (with yet to determine accurate proper motions) or that they are part of an unrecognized cluster or star forming region. The primary cause for the unknown origin of this subgroup of the O stars is that they are generally located far away.

For clarity, in this paper we will make the explicit distinction between field O stars and runaway O stars, in the sense that runaway stars are not considered to be part of the group of field O stars, following the above reasoning.

## 2.2. Catalogues of O stars

Various catalogues of O stars have been compiled over the years. The main O-type star reference catalogue is the ‘‘Catalog of O type Stars’’, hereafter COS82, compiled from literature data by Garmany et al. (1982). It is a volume limited sample out to an estimated distance of  $\sim 2.5$  kpc and contains 765 entries. Table 1 gives some characteristics of the COS82 catalogue and of three other, more recent catalogues. These three catalogues are partly based on the COS82 catalogue. All four catalogues list for every entry the parent association/cluster when known. Using this information, Col. 4 of Table 1 shows the variation of the census of field O stars since 1982. It is reduced greatly by G87 with respect to COS82, and remains quite stable at a fraction of  $\sim 20\%$  thereafter. The massive field star fraction from the M98 catalogue is given as function of spectral subtype in Fig. 1. This fraction does not show a systematic dependence on spectral type, which implies that if isolated massive star

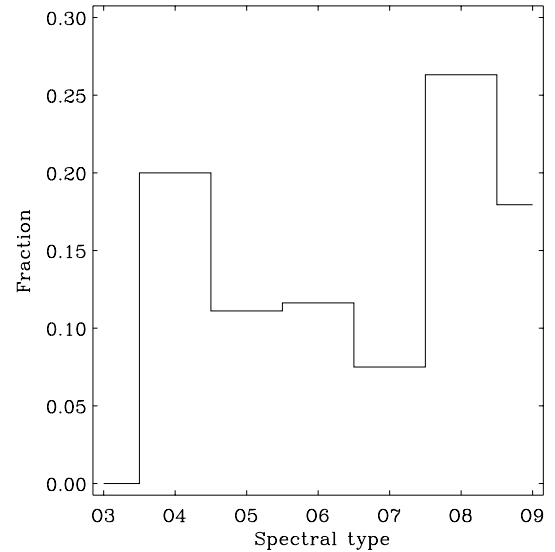


**Fig. 1.** The fraction of field O stars to the total number of O-type stars as function of spectral subtype, adopted from the M98 sample. Considering the small numbers, the fraction of field O stars seems independent of spectral subtype.

formation in the Galaxy existed, the corresponding IMF would be similar to the one in clusters. Small differences in total number of entries between the G87, M98 and M04 catalogues consist in O stars for which a clusters/association membership was established over the years and for instance in the inclusion of O-type stars with Wolf-Rayet secondaries (not included in M04, while 5 such systems are included in M98). Finally, we mention that the difference between field O stars and runaway O stars as laid down in the previous paragraph is not the common definition used in these 4 catalogues. Therefore the field star numbers in Col. 4 of Table 1 may include runaway stars.

In Table 1 we have not included the catalogue of Cruz-González et al. (1974). Although the catalogue gives many characteristics of its 664 entries, the catalogue does not specify memberships since it primarily focuses on H II regions and the ionization of the interstellar medium.

## 2.3. Sample selection

In the present study we select the 43 field O stars from the M98 study, that contain 39 stars with  $V < 8^m$  (see Table 1), plus 4 additional fainter objects. These authors search for nearby ( $0.035'' < \rho < 1.5''$ ) companion stars to the target objects using speckle interferometry. They reach the following conclusions with regard to the field O stars: at least 35% contains a secondary object (spectroscopic or visual), and 2 objects are visually multiple systems. Table 2 specifies spectral type, visual magnitude, distance, spectroscopic and visual multiplicity status for each of the field O star in M98, sorted on HD number. The following abbreviations are used for the spectroscopic status: C = constant radial velocity (20 stars), SB1 = single-line spectroscopic binary (8 stars), SB2 = double-line spectroscopic binary (7 stars). Addition of the letter ‘‘O’’ indicates that the orbit is known (6 stars), an ‘‘E’’ indicates eclipsing

systems (6 stars). A colon has the usual meaning of uncertainty. For the visual multiplicity status in Col. 6, following G87, we use OPT = optical binary (5 stars), VB = visual binary (6 stars), VMS = visual multiple object (2 stars) and single O-type field stars (30 stars).

The M98 study is an update of the study by G87. Therefore the M98 census of the 43 field O stars nearly equals the G87 census. For completeness reasons we point out that the M98 sample differs by four objects with G87, that were in fact discovered to be member of a cluster or association, viz. HD 5005, HD 14947, HD 47432, HD 71304.

We now give a short description of how the O star field sample is compiled with respect to identification of parent clusters. The O-type star sample of G87 is constructed primarily from the LSC catalogue (Humphreys & McElroy 1984), selecting stars with  $V < 8^m$ . In turn, the main O-type star input of the LSC is the COS82. The cluster/association membership for the stars is obtained by cross-correlating the LSC with the clusters and associations as catalogued by Alter et al. (1970) and Ruprecht et al. (1981). The *runaway* O stars in the M98 sample are defined using one of three separate criteria: (1) having either a peculiar radial velocity greater than  $30 \text{ km s}^{-1}$ ; (2) a peculiar space velocity greater than  $30 \text{ km s}^{-1}$ ; or (3) stars with a distance from the Galactic plane greater than 500 pc. Finally, 43 O-type stars in the M98 sample are not members of a cluster and are not runaway stars. They are annotated as *field* stars. We would like to note that the field O star population defined in this way contains three confirmed runaway stars, viz. HD 66811 ( $\zeta$  Pup, e.g., Chlebowski 1989), HD 75222 (Hoogerwerf et al. 2001) and HD 153919 (Ankay et al. 2001). We have marked them in Table 2 with an asterisk.

As a final note on the M98 field O star census, we would like to point out the existing confusion concerning the visual binary star HD 48149. The star is characterized in the M98 sample as a field O8.5V star. However, according to SIMBAD, it is a G2/G3V star. SIMBAD gives the extra note that confusion exists between this star and HD 46149, an O8.5V star in the cluster NGC 2244. We do not consider HD 48149 as an O-type star in this paper.

### 3. Observations and search method

#### 3.1. ESO/NTT, INAF/TNG and 2MASS

The 43 field O stars from the M98 census were observed with the NTT at the ESO LaSilla facility and with the Telescopio Nazionale Galileo (TNG). The TNG is Italy's 3.5 m optical/infrared telescope, operated from the Roque de los Muchachos on La Palma (Canary Islands). It has an alt-azimuth mount and Ritchey-Chretien configuration with two Nasmyth foci and active optics control.

At the NTT the stars were observed with the SOFI instrument, whereas the TNG was equipped with NICS (Near Infrared Camera Spectrometer) camera. The field of view (FoV) and resolution using these cameras are very similar,  $5 \times 5$  arcmin and  $\sim 0.3$  arcsec/pixel, respectively. In Fig. 2 we show the distribution of the projected linear scale of the FoV of SOFI and NICS for the adopted distances listed in Table 2.

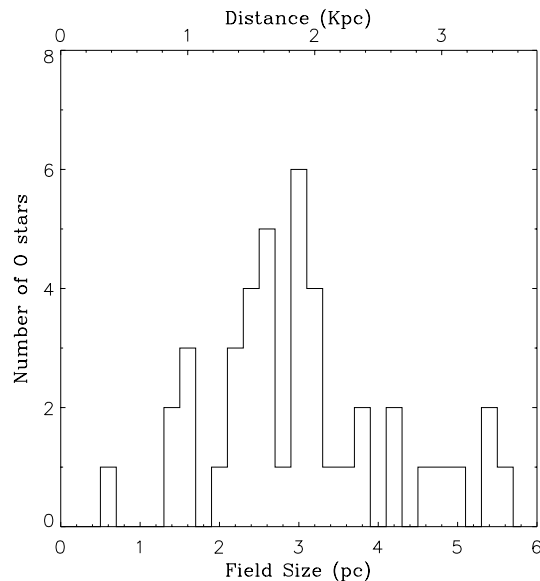


**Fig. 2.** Distribution of distances of target O-type stars and the corresponding sizes of the field of view.

NTT and 2MASS imaging was performed in the NIR K-short filter ( $\lambda_c = 2.16 \mu\text{m}$ ) and TNG imaging in the *K*-prime filter ( $\lambda_c = 2.12 \mu\text{m}$ ), using standard dithering strategy for background subtraction purposes. The *K*-band was chosen to minimize the difference in magnitude between the bright O-type star and the surrounding stellar population. Images were bias-subtracted, flat-fielded and combined using NOAO/IRAF data reduction software. Source extraction and aperture photometry was done with the DAOPHOT routines running under IDL.

The central O-type stars are in all cases saturated, because long exposure times were used to pick up the faintest stars. The saturated profile is highly non-linear and shows features that are identified by DAOPHOT as candidate stars. Meticulous care is taken in source identification close to the saturated target O-type stars. To prevent false detections, we compare different saturated PSFs of the central O stars and other bright stars in the field to identify the general PSF features. Such exercises result generally in rejection of features dimmer than  $\Delta K \gtrsim 8^m$  within a radius of 5 arcsec from the target O star.

To probe larger fields in search for clusters around field O stars, we use the recently released 2MASS All Sky Data Release. Catalogues spanning  $20 \times 20$  arcmin were extracted from the Point Source Catalog (PSC)<sup>1</sup> and analyzed in the same way as the NTT and TNG data. The PSC is 99% complete for  $K_s < 14.3^m$ , however we use for each 2MASS field the proper completeness limit (see Col. 10 of Table 2).

#### 3.2. Counting method

The images are analyzed for stellar density enhancements, by counting and binning methods. In each field the detected stars are binned in subfields. For the deeper TNG and NTT images, we choose a binning resolution of  $11 \times 11$  subfields. The shallower but larger 2MASS fields are all subdivided in

<sup>1</sup> From <http://www.ipac.caltech.edu/2mass/>

15 × 15 subfields. The binning grid is chosen so that the target O-type star falls in the centre of one of the subfields. Then, the average stellar density is calculated and the corresponding Poisson standard deviation compared with the number of detected stars in each subfield. A  $3\sigma$  offset from the average is considered to be a possible cluster of stars, although it could still be compatible with the Poisson distribution of the number of stars per subfield. Whenever the  $3\sigma$  detection also happens to be centred on the target star, its physical association is inferred.

Only stars brighter than the completeness limit are taken into account. The completeness limits (Cols. 9 and 10 in Table 2) differ from frame to frame due to crowding and observing conditions. The exposure time is the same for each field. The density maps are presented in Sect. 4 with overlaid contours indicating the offset in standard deviations, starting at  $1\sigma$  from the mean density of the complete field. We note that the density maps have different linear resolutions, because the binning is chosen the same for each field. Therefore 2MASS maps have linear resolutions between 0.5 pc and 2 pc, whereas the TNG and NTT maps between 0.15 pc and 0.5 pc. The linear resolutions of the density maps are comparable to the sizes of stellar clusters. The maps are smoothed for presentation purposes. Some maps show white, low-density regions near bright, saturated stars (e.g. HD 91452 or HD 125206) and also near some of the target stars. This is caused by the extended and highly non-linear PSF of saturated objects in the SOFI and NICS images.

#### 4. O-type field stars; visually single or in clusters?

In this section we present the *K*-band images, the stellar densities maps on small (NTT and TNG) and large scales (2MASS), and a description of each object. The description focuses on the currently known visual multiplicity status of the field O stars and nearby early-type (<B5) stars. Special attention is given to nearby young clusters taken from the literature and/or from WEBDA<sup>2</sup>. Specifically, we searched for known stellar clusters with ages less than 10 Myr located within a projected distance less than 65 pc as calculated from the distance of the field O star. The average peculiar radial velocity of field O stars is  $\sim 6.4 \text{ km s}^{-1}$  (G87), therefore during a lifetime of  $\sim 10^7$  years, the field O stars may wander about  $\sim 65$  pc from their birthplace. In the case that such a cluster exists, and its distance from the Sun is similar to the field O stars' distance within the uncertainty, we list its basic characteristics in a “mini table” added to the description of that particular star. We adopting an uncertainty of 30% on the distances for the O stars. The stars are presented in this section ordered by their HD number.

Beforehand we'd like to note that in nearly all cases, the 2MASS maps  $3\sigma$  “detection” show no other indications for a physical cluster, e.g. bright stars or nebulosities either from DSS images or after cross-correlation with the SIMBAD database. These detections are probably purely statistical. The two exceptions are HD 48279 (Fig. 4, a new 2MASS cluster detected on the edge of the considered field) and HD 52533

(Fig. 5, a 2MASS cluster centred on the target star). For every object in the following list, we classify a density peak by stating whether it is a *physical* as opposed to *statistical* cluster depending on whether it is associated with the above mentioned secondary indicators.

##### 4.1. HD 1337 ( $\equiv$ AO CAS)

The massive eclipsing binary AO Cas (O9.5 III + O8 V, Bagnuolo & Gies 1991) is a well studied system that shows the signatures of colliding winds in UV spectra (e.g., Gies & Wiggs 1991). The system is associated with the ROSAT Faint Source Catalogue source 1RXS J001747.4+512549 (Voges 2000). Uncertain spectroscopic distance determinations place it between 1.2 kpc (Stone 1978), 2.1 kpc (M98), and 3.9 kpc (Cruz-González et al. 1974). For the latter distance scale, HD 1337 would be 750 pc below the Galactic plane. There are no young clusters within a projected radius of 65 pc for the adopted distance of 2.1 kpc.

*Our result:* The stellar density maps in the middle and right panel of the top row in Fig. 3 do not indicate a cluster near HD 1337.

##### 4.2. HD 15137

The object is visually a single star and spectroscopically a double-line binary candidate (Conti & Ebbets 1977; Howarth et al. 1997). There is an IRAS source (IRAS 02245+5217) located at 2 arcmin ( $\sim 2$  pc) south of HD 15137, that could be part of a larger loop-like structure visible on the IRAS 60  $\mu\text{m}$  image. No young stellar clusters or stars earlier than B5 are reported within a 65 pc radius from HD 15137.

*Our result:* The stellar density maps does not show evidence for a cluster near HD 15137. The two density peaks at coordinate offset (0, -2) in the TNG density map (second row in Fig. 3) are associated with an IR source and could therefore be a physical cluster. This cluster is however not detected on the 2MASS map.

##### 4.3. HD 36879

Spectroscopically, the star is a single object that is found to have unexpectedly narrow Si IV lines in its IUE spectra by Walborn & Panek (1984). These stellar wind lines change significantly in the course of 4 days. The presence of narrow Si IV and C IV absorption are preferentially seen towards O-type stars in cluster and/or nebulosities (de Kool & de Jong 1985). These lines are thought to be due to slowly evaporating clouds within the stellar wind bubble. Interestingly, an isolated T Tauri star is reported to be located at a distance of  $\sim 10$  pc by Li & Hu (1998). The nearest early type star is HD 245310, a B2 object, at a projected distance of  $\sim 7$  pc. No clusters are found within 65 pc radius from the target star.

*Our result:* The NTT  $K_s$ -band image shows that HD 36879 consists of two objects with a separation of  $9''.6$  and  $\Delta K = 1.2^m$ . HD 36879 is therefore either a visual or an optical binary. Cross-check with 2MASS finds that the companion object has

<sup>2</sup> <http://obswww.unige.ch/webda/navigation.html>

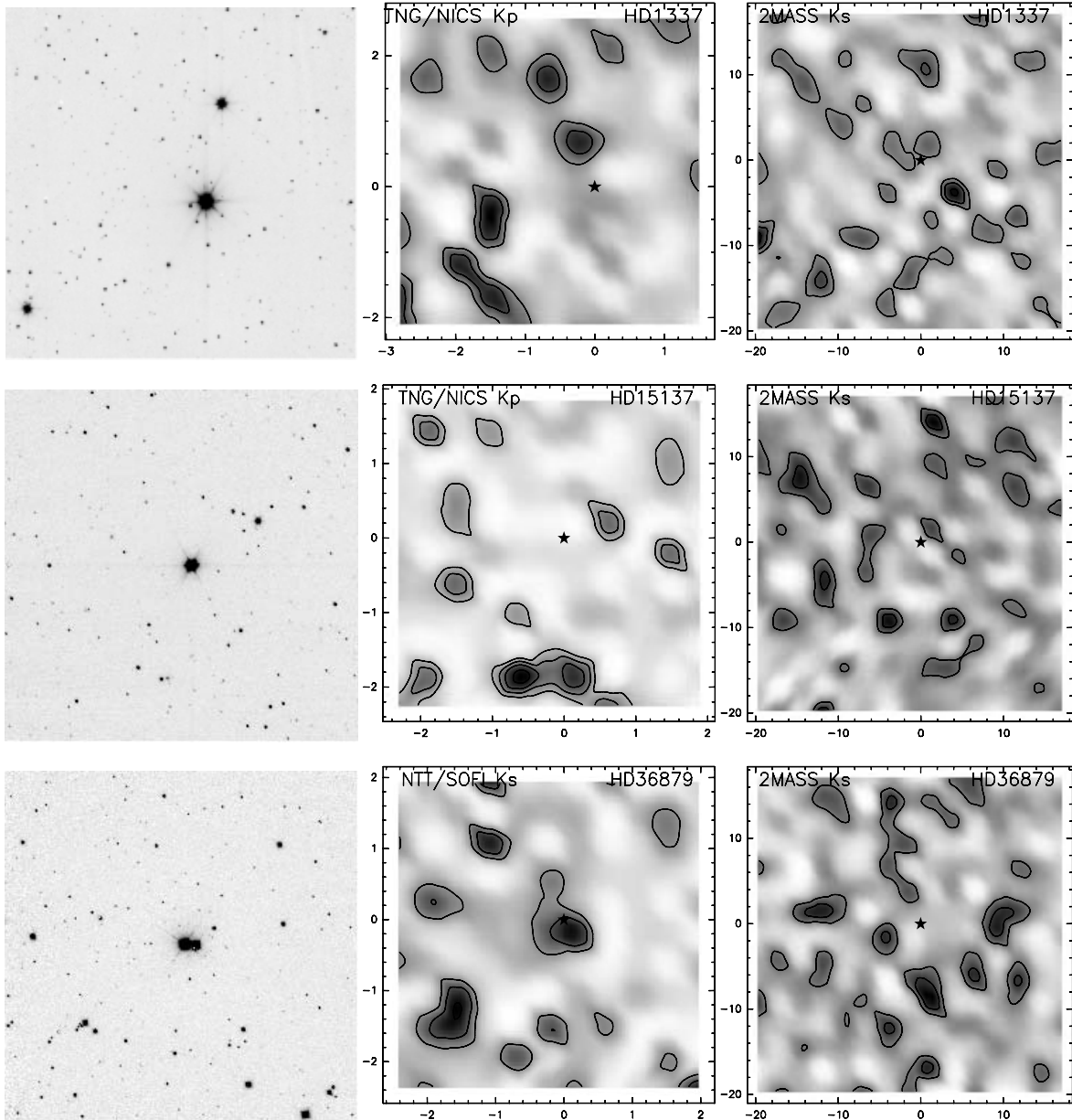


**Fig. 3.** *Left panels:*  $K_s$ -band image with 5 arcmin on a side. *Middle panels:* corresponding surface stellar density maps. *Right panels:* density maps derived from the 2MASS PSC, for stars HD 1337, HD 15137 and HD 36879. Ordinates are in arcmin for the middle and right panels. Contours are  $1\sigma$  spaced deviations from the average stellar density value.

*NIR* colours ( $J - K$ ) = 1.08, indicating a late-type object. The density maps indicate no physical cluster near this star.

#### 4.4. HD 39680

HD 39680 is an emission line star with double peaked Balmer line emission (Gies & Bolton 1986) and an infrared excess which is interpreted as free-free emission originating in the stellar wind. Marchenko et al. (1998) notes the formidable long-term photometric variation of this object resembling classical Be star behaviour. In this sense it is similar to another Oe star in our sample: HD 60848. HD 39680 is an optical binary (Lindroos 1985) whose components were observed by M98 and appeared as single stars. There are no clusters

within 65 pc of HD 39680 and the star is in fact the only O-type star within a radius of 100 arcmin ( $\sim 70$  pc). The closest early type star is at a projected distance of 11 pc, viz. the variable B4 V star Z Ori.

*Our result:* There is no indication of a physical cluster near this object from the density maps in Fig. 4.

#### 4.5. HD 41161

The object forms a visual binary system with the component separated at 9.8 arcsec (M98). Unexpectedly, Noriega-Crespo et al. (1997) report a resolved IR bow shock near this system that would be indicative of large spatial velocities. This visual binary is relatively far from the Galactic plane.

*Our result:* The stellar densities near HD 41161 are low. In the  $K$ -band image of the second row of Fig. 4, the secondary star is detected to the right of HD 41161. The density maps do not reveal any physical cluster near HD 41161.

#### 4.6. HD 48279

The multiple nature of HD 48279 is visible in the left panel of the third row in Fig. 4. This system is likely to be an optical configuration (M 98). The small group of 4 objects is associated with an IR source: IRAS 06400+0146. The target star lies in the field of the Mon OB2 association, which has a comparable but smaller distance of 1.6 kpc (Mel'Nik & Efremov 1995); HD 48279's membership is not clear. The young cluster Dolidze 25 is found within 65 pc of the target star. This cluster however is located at a distance of 6.3 kpc, much further away than HD 48279.

*Our result:* The NTT  $K_s$ -band density map shows no indication of clustering of sources within a projected field of view of 1.4 pc. The 2MASS density map however shows at offset  $(-20, -20)$  a hint of a stellar cluster. A visual inspection of a DSS image reveals a clustering of bright objects at the same location. It appears to be centred on the A 2 star HD 289038.

#### 4.7. HD 52266

The object is a candidate spectroscopic binary. It is projected close to the CMa OB 1 association that has a distance of 1 kpc (Kaltcheva & Hilditch 2000). HD 52266's distance of 1.7 kpc locates it further away. The Hipparcos distance estimate would put HD 52266 at 485 pc with considerable uncertainty.

*Our result:* The high resolution stellar density map in the middle panel of the upper row of Fig. 5 shows evidence for a cluster near the target star. This cluster is not detected on the 2MASS density map.

#### 4.8. HD 52533

The visual multiplicity of the star is clearly visible in the first panel of the second row of Fig. 5. Part of this multiple system (M 98) is the early-type star SAO 134062 and at 50 arcsec the B1 star HD 52504). HD 52533 itself is a single-line spectroscopic binary with a period of 3.3 days (Gies & Bolton 1986). It is associated with a  $60 \mu\text{m}$  excess (Noriega-Crespo et al. 1997) and an unpublished X-ray source (1RXS J070126.3-030704).

*Our result:* Both the density map derived from the  $K_s$ -band NTT image and the 2MASS map in Fig. 5 show a strong indication for clustering of stars near HD 52533.

#### 4.9. HD 57682

HD 57682 is spectroscopically a single object. It is associated with the unpublished X-ray source 1RXS J072201.7-085844 and with the IR source IRAS 07196-0852. The star is reported to be a variable Oe star by Coté & van Kerkwijk 1993 (see also MacConnell 1981). Having a rather small  $v \sin i$  of  $33 \text{ km s}^{-1}$  (Penny 1996), the object's rotational axis is oriented probably

at a near pole-on angle. The object is suggested to be a run-away star by Cameron et al. (1998).

*Our result:* The NTT stellar density map shows signs of a cluster near HD 57682. The 2MASS density map however only gives evidence for a possible cluster centred at offset  $(6, -9)$ . SIMBAD and DSS do not provide additional indications for a cluster at this position.

#### 4.10. HD 60848 ( $\equiv$ BN GEM)

BN Gem is a star of unknown spectroscopic multiplicity status. The object has an emission line spectrum and manifests similar continuum emission variability as classical Be stars (Divan et al. 1983, see also HD 39680) The object has a reported  $v \sin i = 240 \text{ km s}^{-1}$  (Penny 1996). There are no clusters, O-type or early B-type stars within a projected radius of 65 pc from HD 60848.

*Our result:* The stellar density map derived from the NTT image does not show stellar density peaks near this object. The 2MASS density map shows a density peak at offset  $(4, 5)$  that is likely to be statistical.

#### 4.11. HD 66811 ( $\equiv$ $\zeta$ Pup)

$\zeta$  Pup is the nearest O-type star to the sun and a runaway object (e.g., Upton 1973), although its radial velocity is insufficient to be refer to by M 98 and G 87 as such (see Sect. 2.3). It is spectroscopically single and one of the exciting stars of the Gum Nebula (Chanot & Sivan 1983). Identification of  $\zeta$  Pup with a parent cluster/OB-association has failed so far (see Hoogerwerf et al. 2001; Vanbeveren et al. 1998). The star is included for completeness reasons as it is part of the M 98 sample of field O stars.

*Our result:* The density maps show the expected absence of a cluster centred on the star. The NTT/SOFI image has a density peak at an offset of  $(0, -0.6)$ .

#### 4.12. HD 75222

Hipparcos measured this star being a runaway object with a peculiar space velocity of  $57.2 \text{ km s}^{-1}$  (Hoogerwerf et al. 2001). It is listed as a candidate member of the Vel OB1 association by Reed (2000) on the basis of an extinction study. Like  $\zeta$  Pup, the star is included in our study for completeness reasons (see Sect. 2.3).

*Our result:* The density maps show the expected absence of clusters.

#### 4.13. HD 89137

The star is reported to have a peculiar spectrum by Walborn (1976) and was found to be a candidate single-line spectroscopic binary by Levato et al. (1988). The source IRAS 10137-5059 is located at 1.3 arcmin. This object is unresolved at the 1 arcmin resolution IRAS maps of Noriega-Crespo et al. (1997). Extended  $60 \mu\text{m}$  emission is detected by IRAS and comprises also HD 89137.

*Our result:* The stellar density map derived from the NTT image in Fig. 7 shows a strong density peak at offset (1.6, 1.0). This cluster is not associated with any known physical object in SIMBAD.

#### 4.14. HD 91452

The object is spectroscopically a single star, that is located in the direction of the Carina Spiral Feature and at a 1.3 degrees distance from the Theta Carina cluster. HD 91452 suffers from a reasonable extinction of  $A_V \approx 1.5^m$ . There are no known clusters within a projected radius of 65 pc of HD 91452. The nearest early type star is a B5 star HD 307781 at 37 pc.

*Our result:* The stellar density maps do not show any cluster near HD 91452.

#### 4.15. HD 96917

The object is a candidate single-line spectroscopic binary and a known variable star with evidence for photometric micro-variability (Balona 1992). Like HD 91452, HD 96917 is located in the direction of the Carina Spiral Feature. The nearest early-type star is the B2 star HD 96088 at a distance of 51 pc.

*Our result:* The stellar density maps do not reveal any physical cluster.

#### 4.16. HD 105627

HD 105627 is located in a crowded field, but isolated from other O-type stars. The nearest O-type star is in fact at an angular distance of 1.44 degrees (80 pc). It is a relatively little studied star, with an Hipparcos astrometric optical companion at 14 arcsec (M98).

*Our result:* The density maps do not indicate any physical cluster.

#### 4.17. HD 112244

This emission line object is a visual binary from the Lindroos sample (Lindroos 1985). The secondary is a K0III star. Recently, the system was suggested to be an optical configuration (Huélamo et al. 2000). The primary O-type star is a candidate single-line spectroscopic binary. HD 112244 shows regular photometric variability with three possible periods (Marchenko et al. 1998). It is associated with the IR source IRAS 12529-5633 and it is an X-ray source. The closest early type-star is another emission line O star HD 112147, at a projected distance of 57 pc.

*Our result:* The density maps in Fig. 8 do not reveal any physical clustering near HD 112244. The 2MASS map density peaks are likely to be statistical.

#### 4.18. HD 113659

A star with unknown spectroscopic multiplicity status according to M98, although it is reported to have a variable radial velocity and to be a member of the Cen OB1 association

according to the LSC (Humphreys & McElroy 1984; see also Mathys 1988). Therefore this star is a doubtful field O star.

*Our result:* The stellar density map do not show clusters.

#### 4.19. HD 117856

The object is a close visual binary (1.6 arcsec) and a candidate double-line spectroscopic binary. The field shows a collection of interstellar dark clouds and H II regions, that may be part of the Southern Coalsack (distance of 180 pc). With an estimated distance of 1.7 kpc, HD 117856 is probably piercing through the fringes of this star formation region. Stock 16 is a young cluster ~60 pc away and related to the H II region RCW 75. It has a distance of 1.9 kpc (Turner 1985), comparable to that of HD 117856.

*Our result:* The density maps do not reveal any physical clusters.

Cluster name	Ang. dist. (deg)	Lin. dist. (pc)	Age (Myr)	Dist. (kpc)	Ref.
Stock 16	1.9	57	4	$1.9 \pm 0.08$	1

1: Turner (1985).

#### 4.20. HD 120678

The object is a variable emission line star and a rapid rotator with  $v \sin i = 350 \text{ km s}^{-1}$  (Conti & Ebbets 1977). HD 120678 is of unknown spectroscopic multiplicity status. It is located in a crowded field together with two other early-type stars: a B2 star at 4.5 pc (HD 120634), and a B5 star at 3.3 pc (HD 120578).

*Our result:* The stellar density maps do not show any physical cluster.

#### 4.21. HD 122879

Spectroscopically a single star that has been noted as a variable object with a period of 1.58 days based on Hipparcos photometry by Marchenko et al. (1998). The spectral type is probably B0Ia rather than O9.5I as listed in Table 1 (following Garrison et al. 1977; Walborn & Fitzpatrick 1990). The object was suggested to be member of Cen OB1 (e.g., Pawlowicz & Herbst 1980).

*Our result:* The stellar density maps do not show any clustering near this object.

#### 4.22. HD 123056

The object is spectroscopically a single star and not part of the G87 sample of O-type field stars. Little is known about it. An IR source (IRAS 14040-6014) is located at 1.5 arcmin SE of HD 123056.

*Our result:* The stellar density maps do not show a physical cluster near this object.

#### 4.23. HD 124314

The object is a visual binary star with a 2.7 arcsec separation. It is a candidate single-line spectroscopic binary (Feast et al. 1955), although Balona (1992) finds a nearly constant light curve. HD 124314 is an emission line star and the main ionizing source of the H II region RCW 85 (Yamaguchi et al. 1999). It is associated with the ROSAT source 1RXSJ141500.1-614231 and the IR source (1.5 arcmin NW) IRAS 14111-6127. The young cluster NGC 5606 is at a projected linear distance of  $\sim 45$  pc, but roughly twice as far from the sun than HD 124314.

*Our result:* The density maps do not reveal any stellar cluster associated with this star.

#### 4.24. HD 125206

A candidate double-line spectroscopic binary. The star is located  $\sim 10$  pc north of the star forming H II region RCW 85 (see Yamaguchi et al. 1999). This region is at a similar distance as HD 125206. Mel’Nik & Efremov (1995) note that HD 125206 may belong to their *Clust 3* group. HD 125206 is at a distance comparable to the one of the young cluster NGC 5606. The projected distance between these two objects is less than 65 pc.

*Our result:* The stellar density maps do not show an indication of a cluster near HD 125206. The 2MASS density peak at offset  $(-12, 7)$  in Fig. 10 could be associated with the IR source IRAS 14183-6044. Another stellar density peak at offset  $(12, -17)$  lies close to the IR source IRAS 14143-6108.

Cluster name	Ang. dist. (deg)	Lin. dist. (pc)	Age (Myr)	Dist. (kpc)	Ref.
NGC 5606	1.7	51	7	$2.4 \pm 0.2$	1

1: Vazquez et al. (1994).

#### 4.25. HD 135240

This double-line ellipsoidal spectroscopic binary is shown to be a massive triple system consisting of O7III-V, O9.5V, and B0.5V stars (Penny et al. 2001). The primary and secondary have different evolutionary ages of 2.5 Myr and 5.1 Myr, respectively. The source is associated with the X-ray source 1RXS J151658.5-605730. Another early-type Be star (HD 135160) is located at 1 pc. A third early-type B3 star is at a distance of 1.3 pc. HD 135240 may belong to Mel’Nik & Efremov’s (1995) *Pis 20* group.

*Our result:* The density maps do not indicate any cluster near this triple system.

#### 4.26. HD 135591

A triple object of which the third component is located at 44.5 arcsec (Lindroos 1985). The latter is an A8III star, that would still be in the pre-main sequence phase. HD 135591

is also associated with the X-ray source 1RXSJ151848.4-602952. This system may belong to Mel’Nik & Efremov’s (1995) *Pis 20* group. There are a number of nearby early-type stars, e.g. HD 135786 at  $\sim 3$  pc, but known young clusters are absent within 65 pc radius.

*Our result:* There is no indication of a cluster near this star.

#### 4.27. HD 153426

The object is a candidate double-line spectroscopic binary and located within a half degree of the H II region Sharpless 2. It was suggested by Walborn (1973) that the object could be physically related to the runaway HMXB HD 153919/4U1700-37 (see Ankay et al. 2001), that is at a projected linear distance of  $\sim 24$  pc. Note that SIMBAD lists HD 153426 wrongly as a B9II-III star.

*Our result:* The density map in Fig. 11 derived from NTT imaging shows the target star associated with a clear density peak. Although HD 153426 is offset from the cluster centre, we consider the density peak as a physical cluster.

#### 4.28. HD 153919

The object is a single-line eclipsing spectroscopic binary and known as the runaway HMXB 4U1700-37 (Ankay et al. 2001). The object is located in the field of the open cluster NGC 6281, also known as NGC6281-2. It is included in this survey for completeness reasons as it is part of the M98 subsample of O-type field stars (see Sect. 2.3).

*Our result:* The density maps show the expected absence of clusters near the object.

#### 4.29. HD 154368

HD 154368 is a visual binary and an eclipsing binary with a 16.1 day period, located near the Sco OB 1 association. The spectroscopic distance estimate is 800 pc (Snow et al. 1996). The Hipparcos parallax measurement allows an uncertain distance estimate of 370 pc. HD 154368 is mainly known for a translucent cloud in its direction. Its coordinates puts it within the error ellipse of the IR source IRAS 17031-3522. The young cluster Bochum 13 is located within 65 pc projected radius. According to Battinelli et al. (1994) the error on the absolute distance modulus can be  $\sim 0.5^m$ . Therefore the distance to the Sun of HD 154368 and Bochum 13 are similar within the adopted errors.

*Our result:* The target star is not found in a cluster on the density maps in Fig. 12.

Cluster name	Ang. dist. (deg)	Lin. dist. (pc)	Age (Myr)	Dist. (kpc)	Ref.
Bochum 13	2.2	42	6.3	$1.7 \pm 0.45$	1

1: Battinelli et al. (1994).

#### 4.30. HD 154643

HD 154643 is a little studied, candidate single-line spectroscopic binary. Within 65 pc, the young cluster Bochum 13 is found. It has an age of 6.3 Myr and a distance of 1.7 kpc (Battinelli et al. 1994). The distance to the Sun of HD 154643 is comparable to that of Bochum 13.

*Our result:* The density maps do not show any indication of a physical cluster.

Cluster name	Ang. dist. (deg)	Lin. dist. (pc)	Age (Myr)	Dist. (kpc)	Ref.
Bochum 13	1.9	44	6.3	1.7 ± 0.45	1

1: Battinelli et al. (1994).

#### 4.31. HD 154811

HD 154811 is most likely a single component supergiant (Levato et al. 1988). An uncertain Hipparcos distance would put it at 0.42 kpc. An IR source (IRAS 17060-4657) is located at 1.5 arcmin from HD 154811, but the star falls outside the IRAS error-ellipse.

*Our result:* Although the NTT  $K_s$ -band image in Fig. 13 shows some conspicuous bright stars, both density maps do not reveal any clustering near the star. Whether this group of stars is associated to the field O star is unlikely, as 2MASS data shows that a number of them are bright  $K$ -band objects with  $J - K > 1.5$ , occupying the gaint branch region in a colour-magnitude diagram. This suggests that these are evolved low-mass stars.

#### 4.32. HD 158186

This field star is a binary system whose eclipsing Hipparcos light curve was presented by Marchenko et al. (1998). The field itself shows signs of active star formation. HD 158186 is associated with an unresolved IR source IRAS 17260-3129 (Noriega-Crespo et al. 1997). The centre of the dark cloud LDN 1732 coincides with the position of the target star, which could also be the illuminating source of the close by H II region BBW 32300. On angular scales of 40 arcmin, clear nebulosities and obscured regions are distinguishable from optical images, among which the emission nebulae Sh 2-13 and RCW 133. Three young clusters are found within a projected radius of 65 pc, among which NGC 6383 belonging to Sgr OB1 association with an estimated age of 1.7 Myr. NGC 6383 is at 1.5 kpc from the Sun (Fitzgerald et al. 1978), comparable to HD 158186's distance.

*Our result:* The density maps in Fig. 13 do not show a cluster near the target star.

Cluster name	Ang. dist. (deg)	Lin. dist. (pc)	Age (Myr)	Dist. (kpc)	Ref.
NGC 6383	1.6	30	1.7	1.5 ± 0.2	1

1: Fitzgerald et al. (1978).

#### 4.33. HD 161853

The target star is a candidate single-line spectroscopic binary and the exciting star of the H II region RCW 134 (Yamaguchi et al. 1999). The object has been listed as a candidate PN (Ratag et al. 1990) based on its IRAS colours and radio continuum emission. HD 161853 is also associated with the X-ray source 1RXS J174916.5-311509. Within 65 pc radius there is the stellar cluster Collinder 347 with an age less than 10 Myr. Collinder 347 has a distance of 1.5 kpc, comparable to that of HD 161853.

*Our result:* The density map derived from the NTT image in the bottom row of Fig. 13 does not reveal a cluster near HD 161853. The stellar density map derived from 2MASS shows the effect of large scale extinction in the field. Although in a star formation field, HD 161853 does not seem to be associated with a cluster.

Cluster name	Ang. dist. (deg)	Lin. dist. (pc)	Age (Myr)	Dist. (kpc)	Ref.
Collinder 347	2.0	55	6.3	1.5 ± 0.35	1

1: Battinelli et al. (1994).

#### 4.34. HD 163758

The object is a single component Wolf-Rayet star located in an average stellar field. The closest early-type star to HD 163758 is the B 2 object HD 163924 at ~25 pc. No young clusters are found within 65 pc radius.

*Our result:* The density maps do not reveal any cluster near the target star.

#### 4.35. HD 165319

HD 165319 is projected on the ~23 × 23 arcmin H II region RCW 158 (Rodgers et al. 1960). The object suffers from some extinction, showing a colour excess of  $E(B - V) = 0.79$  (Winkler 1997). It is therefore likely associated with, or located further than RCW 158. A second rather extincted O-type star (ALS 4657) is located at ~18 pc distance. No young clusters reside within a projected distance of 65 pc.

*Our result:* A physical cluster is not detected from the density maps.

#### 4.36. HD 169515 (≡ RY Sct)

RY Sct is a well-known double-line massive eclipsing binary. The object is surrounded by a young compact nebula (<2'')

with an unusual geometry, including a concentric set of ionized rings (Smith et al. 1999). HD 169515 is located in a field containing a number of dark clouds, masers and H II regions. The high-mass protostellar candidate IRAS 18223-1243 is located at +5 arcmin east. Therefore the field shows evidence for active star formation. The cluster NGC 6604 is a young object with an age of 4 Myr and a distance of 1.1 kpc in Sharpless 2-54 (Battinelli et al. 1994). The cluster’s distance to the Sun is comparable to that of HD 169515.

*Our result:* The high resolution density map in Fig. 14 does not reveal a cluster near HD 169515. The 2MASS map in the bottom right panel has a rather structured stellar density distribution due to large scale extinction on the west side of the map. Therefore the density “peak” on the 2MASS map near HD 169515 is not unambiguously identified as a physical cluster.

Cluster name	Ang. dist. (deg)	Lin. dist. (pc)	Age (Myr)	Dist. (kpc)	Ref.
NGC 6604	1.9	65	4	1.1 ± 0.3	1

1: Battinelli et al. (1994).

#### 4.37. HD 175754 and HD 175876

HD 175754 and HD 175876 are described together. Their similarities led Walborn & Fitzpatrick (2000) to suggest that they are physically related.

HD 175754 is an emission line star and a single object, both optically and spectroscopically. It is located 400 pc below the Galactic plane. HD 175876 is an optical binary from the Lindroos sample (Lindroos 1985), located at  $z \approx -420$  pc. The two O-type stars have an angular separation of 1.3 degrees, that translates to  $\sim 50$  pc. Both objects could be related to the “blowout” observed in the Scutum Supershell (Callaway et al. 2000).

*Our result:* The density maps do not reveal clusters near HD 175754 and HD 175876.

#### 4.38. HD 175876

See Sect. 4.37

#### 4.39. HD 188209

The object has a relatively large distance from the Galactic plane ( $z \approx -330$  pc) and is classified as a candidate runaway star by Stone (1979) on the basis of a large ( $>40 \text{ km s}^{-1}$ ) peculiar space velocity. A number of studies have searched for a binary nature of HD 188209, which is suggested by its intricate line-profile variations (e.g., Fullerton et al. 1996). Recently taken echelle spectra detect a 6.4 days period (Israelian et al. 2000), however the authors choose not to infer a binary nature from these measurements. HD 188209 is associated with the X-ray source 1RXS J195159.2+470133. No young

clusters within 65 pc from HD 188209 are known. Closest early type star is the B0.5 III star HD 188439 at 28 pc distance.

*Our result:* The surface density maps do not reveal a cluster near the star.

#### 4.40. HD 193793

The object is a triple system consisting of a 6 arcsec visual binary and the spectroscopic WR-O binary WR 140. A system prototypical for colliding wind phenomena (Monnier et al. 2002), it shows periodical dust formation when close to periastron (e.g., Williams 1996). Optically, the field of HD 193793 shows clear evidence for wisps of ionized gas. IRAS  $60 \mu\text{m}$  imaging shows the field in the interior of a ring-like IR emission structure.

*Our result:* The density maps do not reveal a cluster near this star.

#### 4.41. HD 195592

HD 195592 is an emission line star which is located in the Cygnus X region. The region contains swirls of interstellar ionized gas (see Dickel et al. 1969) and shows the presence of dust extinction. Noriega-Crespo et al. (1997) identified an IRAS bow shock near this star. We mention two young clusters in the mini-table that, although without age estimates, are likely to be very young as they are thought to be the driving source of massive outflows (see Itoh et al. 1999; Hodapp 1994). However both SF region seem to be located further out into the Galaxy.

*Our result:* The high resolution density map from TNG imaging in Fig. 16 indicates the presence of a cluster near HD 195592. This cluster is however not detected on the 2MASS density map.

Cluster name	Ang. dist. (deg)	Lin. dist. (pc)	Age (Myr)	Dist. (kpc)	Ref.
W 75N IR Cluster	2.2	54	–	2.0	1
DR 21	2.5	61	–	3.0	2

1: Hodapp (1994); 2: Itoh et al. (1999).

#### 4.42. HD 201345

HD 201345 is located at a distance of  $z \approx -300$  pc below the Galactic plane and has a relatively high peculiar radial velocity of  $29.5 \text{ km s}^{-1}$  reported by Gies & Bolton (1986). The star’s photosphere shows evidence for enhanced nitrogen abundance (Walborn 1976). There are no clusters nor early type ( $<B 5$ ) stars known within 65 pc of the object for our adopted distance of 1.9 kpc.

*Our result:* We find no indication of a cluster from the density maps near the star.

#### 4.43. HD 202124

Spectroscopic measurements show that HD 202124 is likely to be a single object. It is located in the direction of the Cygnus superbubble, a structure related to the OB associations located along the Orion local spiral arm (see Uyaniker et al. 2001). Despite this, there are no young cluster known within 65 pc from HD 202124. An early B2 type star is found at  $\sim 30$  pc (HD 202253).

*Our result:* The stellar density maps do not reveal any cluster near the target star.

### 5. Summary

In this first contribution of two papers on massive O-type field stars, we have presented and discussed stellar density maps derived from *K*-band imaging. The maps were used to search for stellar clusters near 43 target field stars in order to test the hypothesis whether massive field stars are actually members of yet unrecognized clusters. The O-type field star sample is adopted from the paper by Mason et al. (1998). Searches for relatively small scale clusters ( $\sim 0.25$  pc) were executed using deep *K*-band observations, generally with sub-solar mass completeness limits. Larger cluster sizes ( $\sim 1$  pc) were probed using the 2MASS All Sky Data Release. In general, the presented density maps show that the O-type field stars are not residing in clusters. Only in a few instances the maps indicate the presence of stellar density peaks near the target stars. The stars which we found in a cluster are: HD 52266, HD 52533, HD 57682, HD 153426, and HD 195592. The best of these cases is for stars HD 52533 and HD 195592.

The main result of this paper being the general absence of stellar clusters near the massive field O stars is compatible with the suggestion made by Gies (1987). The author lists a number of statistical arguments why the sample of O-type field stars is not compatible with a formation origin in situ. The arguments are based on the kinematical, binary and spectral type statistics of the O-type stars compared to similar stars in clusters/associations and the O-type runaway stars. According to Gies, the O-type field stars could constitute the low velocity tail of the velocity distribution due to dynamical ejection from young stellar clusters. To investigate this in more detail, the accompanying paper (de Wit et al. 2004) will extend the discussion in light of the main result of this paper and use additional information on spatial velocities, association with nearby young clusters and star formation regions in order to constrain the origin of the massive O-type field stars.

*Acknowledgements.* W.J.D.W. acknowledges financial assistance from the European Union Research Training Network “The Formation and Evolution of Young Stellar Clusters” (RTN1-1999-00436). This research has made use of the Simbad database, operated at the Centre de Données Astronomiques de Strasbourg (CDS), and of NASA’s Astrophysics Data System Bibliographic Services (ADS). This publication makes use of data products from the Two Micron All Sky Survey, which is a joint project of the University of Massachusetts and the Infrared Processing and Analysis Center/California Institute of Technology, funded by the National Aeronautics and Space Administration and the National Science Foundation.

### References

- Alter, G., Ruprecht, J., & Vanysek, V. 1970, Catalogue of star clusters and associations + supplements
- Ankay, A., Kaper, L., de Bruijne, J. H. J., et al. 2001, *A&A*, 370, 170
- Bagnuolo, W. G., & Gies, D. R. 1991, *ApJ*, 376, 266
- Balona, L. A. 1992, *MNRAS*, 254, 404
- Battinelli, P., Brandimarti, A., & Capuzzo-Dolcetta, R. 1994, *A&AS*, 104, 379
- Blaauw, A. 1961, *Bull. Astron. Inst. Netherlands*, 15, 265
- Bonnell, I. A., Bate, M. R., & Zinnecker, H. 1998, *MNRAS*, 298, 93
- Bonnell, I. A., Vine, S., & Bate, M. R. 2004, *MNRAS*, 349, 735
- Callaway, M. B., Savage, B. D., Benjamin, R. A., et al. 2000, *ApJ*, 532, 943
- Chanot, A., & Sivan, J. P. 1983, *A&A*, 121, 19
- Chlebowski, T. 1989, *ApJ*, 342, 1091
- Comeron, F., Torra, J., & Gomez, A. E. 1998, *A&A*, 330, 975
- Conti, P. S., & Ebbets, D. 1977, *ApJ*, 213, 438
- Cote, J., & van Kerkwijk, M. H. 1993, *A&A*, 274, 870
- Cruz-Gonzalez, C., Recillas-Cruz, E., Costero, R., et al. 1974, *Rev. Mex. Astron. Astrofis.*, 1, 211
- de Kool, M., & de Jong, T. 1985, *A&A*, 149, 151
- de Wit, W. J., Testi, L., Palla, F., & Zinnecker, H. 2004, *A&A*, submitted
- Dickel, H. R., Wendker, H. J., & Bieritz, J. H. 1969, *A&A*, 1, 270
- Divan, L., Zorec, J., & Andriolat, Y. 1983, *A&A*, 126, L8
- Feast, M. W., Thackeray, A. D., & Wesselink, A. J. 1955, *MmRAS*, 67, 51
- Fitzgerald, M. P., Jackson, P. D., Luiken, M., et al. 1978, *MNRAS*, 182, 607
- Fullerton, A. W., Gies, D. R., & Bolton, C. T. 1996, *ApJS*, 103, 475
- Garmany, C. D., Conti, P. S., & Chiosi, C. 1982, *ApJ*, 263, 777
- Garrison, R. F., Hiltner, W. A., & Schild, R. E. 1977, *ApJS*, 35, 111
- Gies, D. R. 1987, *ApJS*, 64, 545
- Gies, D. R., & Bolton, C. T. 1986, *ApJS*, 61, 419
- Gies, D. R., & Wiggs, M. S. 1991, *ApJ*, 375, 321
- Hodapp, K. 1994, *ApJS*, 94, 615
- Hoogerwerf, R., de Bruijne, J. H. J., & de Zeeuw, P. T. 2001, *A&A*, 365, 49
- Howarth, I. D., Siebert, K. W., Hussain, G. A. J., & Prinja, R. K. 1997, *MNRAS*, 284, 265
- Huélamo, N., Neuhäuser, R., Stelzer, B., et al. 2000, *A&A*, 359, 227
- Humphreys, R. M., & McElroy, D. B. 1984, *ApJ*, 284, 565
- Israelian, G., Herrero, A., Musaeff, F., et al. 2000, *MNRAS*, 316, 407
- Itoh, Y., Chrysostomou, A., Burton, M., et al. 1999, *MNRAS*, 304, 406
- Kaltcheva, N. T., & Hilditch, R. W. 2000, *MNRAS*, 312, 753
- Levato, H., Morrell, N., Garcia, B., & Malaroda, S. 1988, *ApJS*, 68, 319
- Li, J. Z., & Hu, J. Y. 1998, *A&AS*, 132, 173
- Lindroos, K. P. 1985, *A&AS*, 60, 183
- MacConnell, D. J. 1981, *A&AS*, 44, 387
- Maíz-Apellániz, J., Walborn, N. R., Galué, H. Á, et al. 2004, *ApJS*, 151, 103
- Marchenko, S. V., Moffat, A. F. J., van der Hucht, K. A., et al. 1998, *A&A*, 331, 1022
- Mason, B. D., Gies, D. R., Hartkopf, W. I., et al. 1998, *AJ*, 115, 821
- Mathys, G. 1988, *A&AS*, 76, 427
- Mel’Nik, A. M., & Efremov, Y. N. 1995, *Astron. Lett.*, 21, 10
- Monnier, J. D., Tuthill, P. G., & Danchi, W. C. 2002, *ApJ*, 567, L137
- Noriega-Crespo, A., van Buren, D., & Dgani, R. 1997, *AJ*, 113, 780
- Pawlowicz, L. M., & Herbst, W. 1980, *A&A*, 86, 68
- Penny, L. R. 1996, *ApJ*, 463, 737
- Penny, L. R., Seyle, D., Gies, D. R., et al. 2001, *ApJ*, 548, 889

- Ratag, M. A., Pottasch, S. R., Zijlstra, A. A., & Menzies, J. 1990, *A&A*, 233, 181
- Reed, B. C. 2000, *AJ*, 119, 1855
- Rodgers, A. W., Campbell, C. T., & Whiteoak, J. B. 1960, *MNRAS*, 121, 103
- Ruprecht, J., Balazs, B. A., & White, R. E. 1981, *Catalogue of star clusters and associations* (Budapest: Akademiai Kiado)
- Smith, N., Gehrz, R. D., Humphreys, R. M., et al. 1999, *AJ*, 118, 960
- Snow, T. P., Black, J. H., van Dishoeck, E. F., et al. 1996, *ApJ*, 465, 245
- Stone, R. C. 1978, *AJ*, 83, 393
- Stone, R. C. 1979, *ApJ*, 232, 520
- Turner, D. G. 1985, *ApJ*, 292, 148
- Upton, E. K. L. 1973, in *The Gum Nebula and Related Problems*, 119
- Uyaniker, B., Fürst, E., Reich, W., et al. 2001, *A&A*, 371, 675
- Vanbeveren, D., van Rensbergen, W., & de Loore, C. 1998, *The brightest binaries*, *Astrophysics and space science library*, 232
- Vazquez, R. A., Baume, G., Feinstein, A., & Prado, P. 1994, *A&AS*, 106, 339
- Voges, W., Aschenbach, B., Boller, T., et al. 2000, *ROSAT All-Sky Survey Faint Source Catalog*
- Walborn, N. R. 1973, *AJ*, 78, 1067
- Walborn, N. R. 1976, *ApJ*, 205, 419
- Walborn, N. R., & Fitzpatrick, E. L. 1990, *PASP*, 102, 379
- Walborn, N. R., & Fitzpatrick, E. L. 2000, *PASP*, 112, 50
- Walborn, N. R., & Panek, R. J. 1984, *ApJ*, 286, 718
- Williams, P. M. 1996, in *Rev. Mex. Astron. Astrofis., Conf. Ser.*, 47
- Winkler, H. 1997, *MNRAS*, 287, 481
- Yamaguchi, N., Mizuno, N., Moriguchi, Y., et al. 1999, *PASJ*, 51, 765
- Yorke, H. W., & Sonnhalter, C. 2002, *ApJ*, 569, 846

# Online Material

**Table 2.** Observations and specification of the O-type field stars as listed in M98. We adopted the spectral types (Col. 2), distance (Col. 4) and spectroscopic status (Col. 5) from M98. The  $V$  magnitudes (Col. 3) are from the GOS<sup>a</sup> compilation of Maíz-Apellániz et al. (2004). Column 6 gives the visual multiplicity status. The following abbreviations are used in Col. 5: C = constant radial velocity, SB1 = single-lined spectroscopic binary, SB2 = double-line spectroscopic binary. Addition of an “O” indicates that the orbit is known, an “E” indicates eclipsing systems. A column indicates uncertainty. In Col. 6 we use OPT = optical binary, VB = visual binary, VMS = visual multiple object. In Col. 9 we give the  $K$ -band completeness limits for each observation and the corresponding mass limit (in  $M_{\odot}$ ). Column 11 gives measured 2MASS completeness limits. An asterisk at the O-type star’s designation indicates a confirmed runaway status.

Name (1)	Sp. type (2)	$V$ (3)	$D$ (4)	Spect. (5)	Vis. (6)	Obs. date (7)	Telescope (8)	$K_{\text{lim}}$ (9)	$M_{\text{lim}}$ (10)	$K_{\text{lim}}^{\text{2MASS}}$ (11)
HD 1337	O9.5III	5.90	2100	SB2OE	single	2001-07-10	TNG	18.0	<0.10	15.0
HD 15137	O9.5II-III(n)	7.87	3400	SB2:	single	2001-11-21	TNG	18.0	0.15	15.0
HD 36879	O7V(n)	7.57	1600	C	single	2001-02-02	NTT	17.0	<0.10	15.0
HD 39680	O6V(n)pevar	7.94	2500	C	OPT	2001-02-02	NTT	17.0	<0.10	15.0
HD 41161	O8Vn	6.77	1500	C	VB	2001-11-21	TNG	18.0	<0.10	15.0
HD 48279	O8V	7.91	2000	C	OPT	2001-02-02	NTT	17.5	<0.10	15.0
HD 52266	O9IV(n)	7.21	1700	SB1:	single	2001-02-02	NTT	17.5	<0.10	15.0
HD 52533	O8.5V	7.70	2000	SB1O	VMS	2001-02-02	NTT	17.0	<0.10	15.0
HD 57682	O9IV	6.42	1600	C	single	2001-02-02	NTT	17.0	<0.10	15.0
HD 60848	O8Vpe	6.85	1900	U	single	2001-03-22	NTT	16.5	0.14	15.0
HD 66811*	O4I(n)f	2.26	450	C	single	2001-02-02	NTT	17.0	<0.10	15.0
HD 75222*	O9.7Iab	7.42	2400	C	single	2001-02-02	NTT	17.0	0.17	15.0
HD 89137	O9.5IIIInp	7.98	3000	SB1:	single	2001-02-02	NTT	17.5	0.18	15.0
HD 91452	O9.5Iab-Ib	7.50	3100	C	single	2000-05-26	NTT	16.5	0.39	15.0
HD 96917	O8.5Ib(f)	7.08	2700	SB1:	single	2000-05-25	NTT	16.5	0.30	15.0
HD 105627	O9II-III	8.14	3200	C	OPT	2000-05-25	NTT	15.5	0.82	15.0
HD 112244	O8.5Iab(f)	5.38	1500	SB1:	VB	2000-05-25	NTT	16.7	<0.10	15.0
HD 113659	O8/9III	8.05	1700	U	single	2001-03-22	NTT	16.5	<0.10	14.0
HD 117856	O9.5III	7.38	1700	SB2:	VB	2000-05-26	NTT	16.5	0.15	14.0
HD 120678	O8IIIInep	7.87	2200	U	single	2001-02-02	NTT	16.5	0.21	13.5
HD 122879	O9.5I	6.43	2100	C	single	2001-02-02	NTT	17.0	0.15	13.5
HD 123056	O9.5V((n))	8.14	1600	C	single	2000-05-25	NTT	16.5	<0.10	14.0
HD 124314	O6V(n)((f))	6.64	1000	SB1:	VB	2000-05-25	NTT	15.5	<0.10	14.0
HD 125206	O9.5IV(n)	7.92	1700	SB2:	single	2001-03-22	NTT	15.5	0.33	14.0
HD 135240	O7.5III((f))	5.08	920	SB2OE	OPT	2001-03-22	NTT	16.5	<0.10	14.0
HD 135591	O7.5III((f))	5.46	1100	C	VMS	2001-03-22	NTT	16.5	<0.10	14.0
HD 153426	O9II-III	7.47	2100	SB2:	single	2000-05-25	NTT	16.2	0.25	14.0
HD 153919*	O6.5Iaf	6.55	1700	SB1OE	single	2001-03-22	NTT	16.5	<0.10	14.0
HD 154368	O9.5Iab	6.13	1100	SBE	VB	2000-05-25	NTT	16.5	<0.10	14.0
HD 154643	O9.5III	7.17	1300	SB1:	single	2001-03-23	NTT	16.5	<0.10	13.5
HD 154811	OC9.7Iab	6.92	1800	C	single	2001-03-23	NTT	17.0	<0.10	14.5
HD 158186	O9.5V	7.00	1100	SBE	single	2001-03-23	NTT	13.0	0.82	12.5
HD 161853	O8V((n))	7.92	1600	SB1:	single	2001-03-23	NTT	13.5	0.91	12.0
HD 163758	O6.5Iaf	7.33	3600	C	single	2001-03-23	NTT	16.5	0.38	13.0
HD 165319	O9.5Iab	7.93	2100	C	single	2000-05-25	NTT	14.0	1.27	13.0
HD 169515	O9.7Ibpevar	9.19	2000	SB2OE	single	2000-05-25	NTT	14.0	1.10	12.5
HD 175754	O8II((f))	7.02	2700	C	single	2000-05-25	NTT	17.0	0.19	15.0
HD 175876	O6.5III(n)	6.94	2300	C	OPT	2000-05-25	NTT	16.0	0.29	15.0
HD 188209	O9.5Iab	5.63	2000	C	single	2001-07-07	TNG	18.4	<0.10	15.0
HD 193793	O5	6.88	1300	SB2O	VB	2001-07-07	TNG	18.4	<0.10	15.0
HD 195592	O9.7Ia	7.08	1400	SB1:	single	2001-07-06	TNG	18.0	<0.10	15.0
HD 201345	ON9V	7.66	1900	C	single	2001-07-07	TNG	18.4	<0.10	15.0
HD 202124	O9.5Iab	7.81	3500	C	single	2001-07-07	TNG	18.4	<0.10	15.0

<sup>a</sup> <http://www-int.stsci.edu/~jmaiz/GOSmain.html>

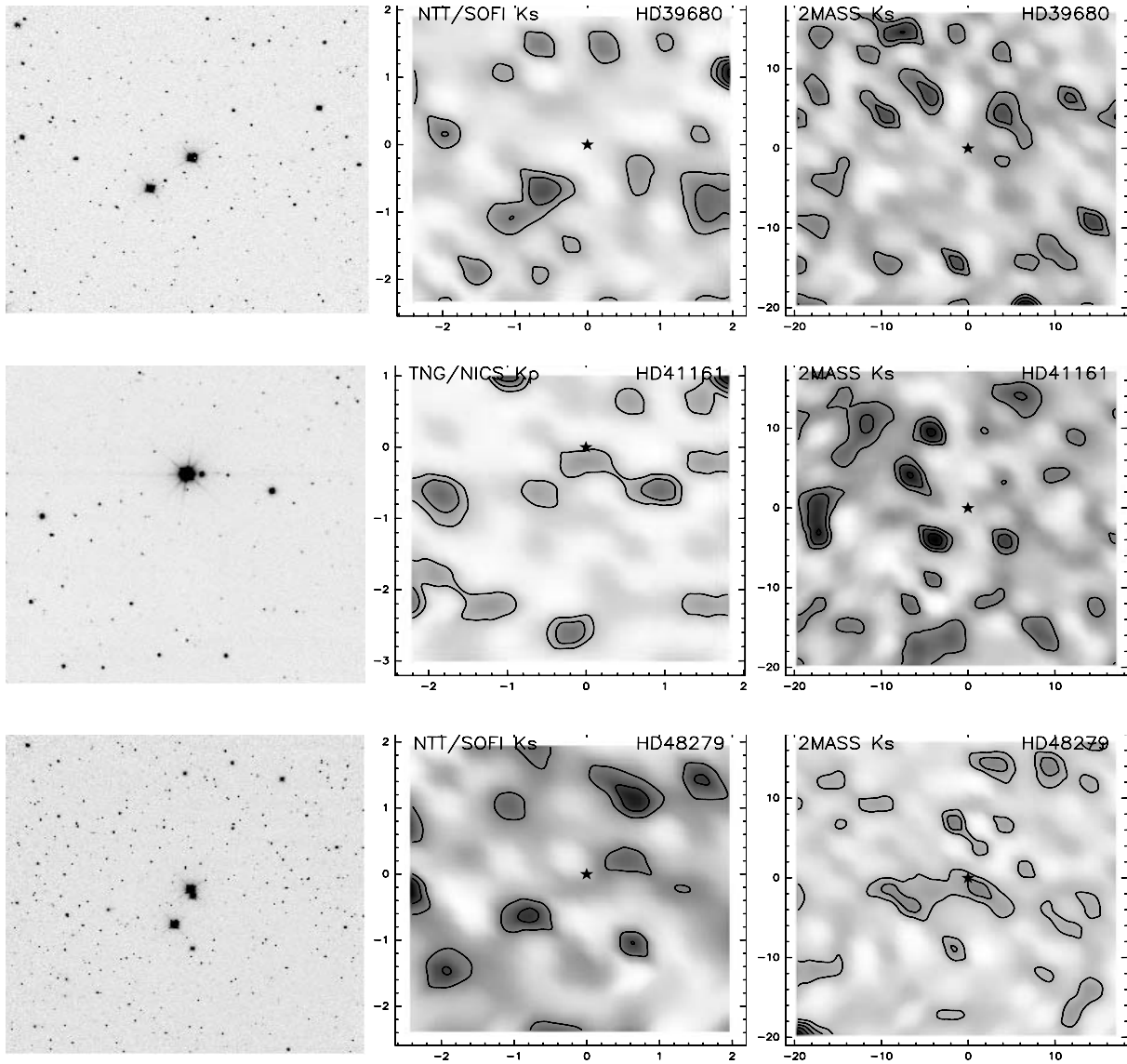


**Fig. 4.** As in Fig. 3 for stars HD 39680, HD 41161, and HD 48279.

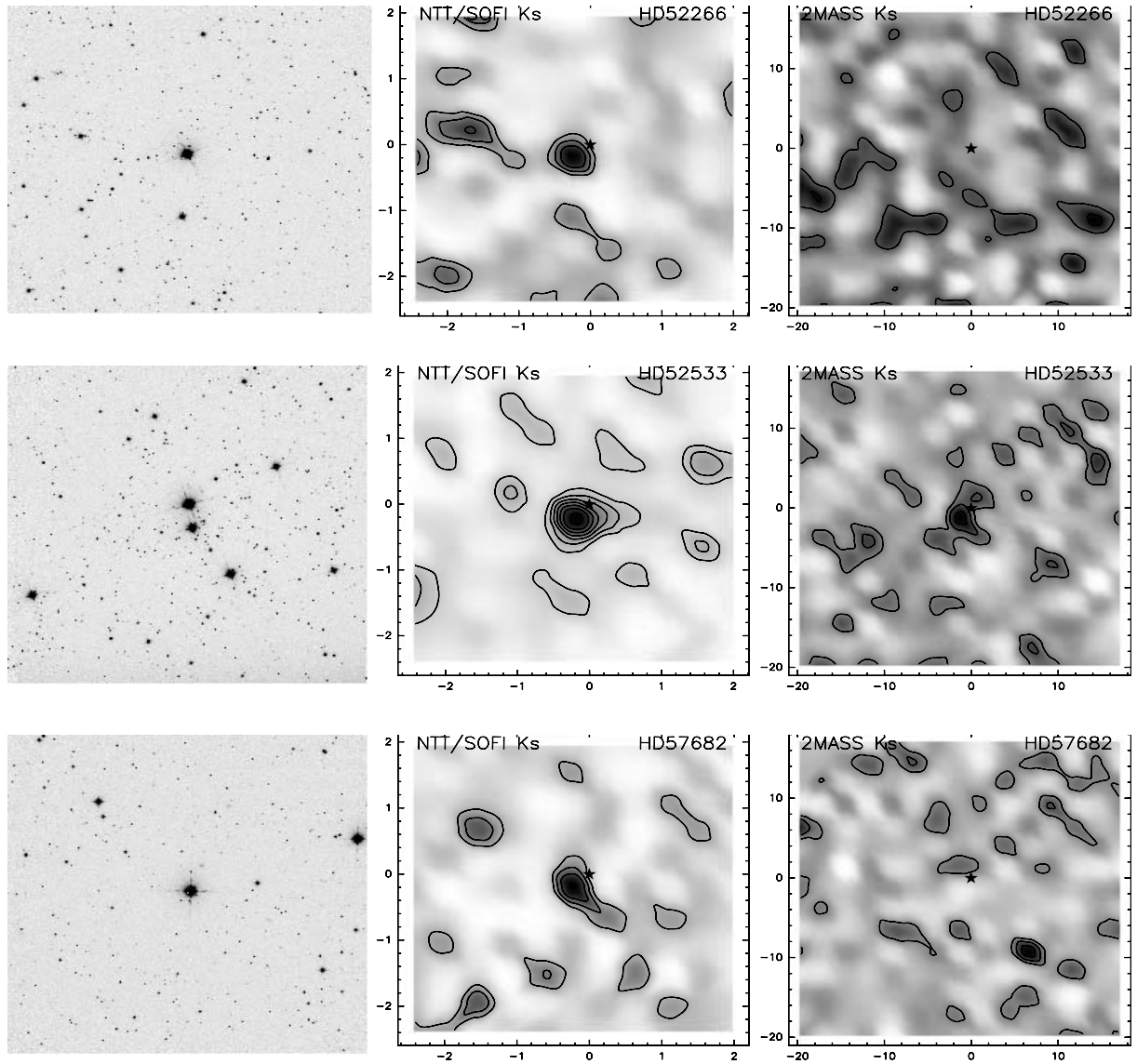


**Fig. 5.** As in Fig. 3 for stars HD 52266, HD 52533, and HD 57682.

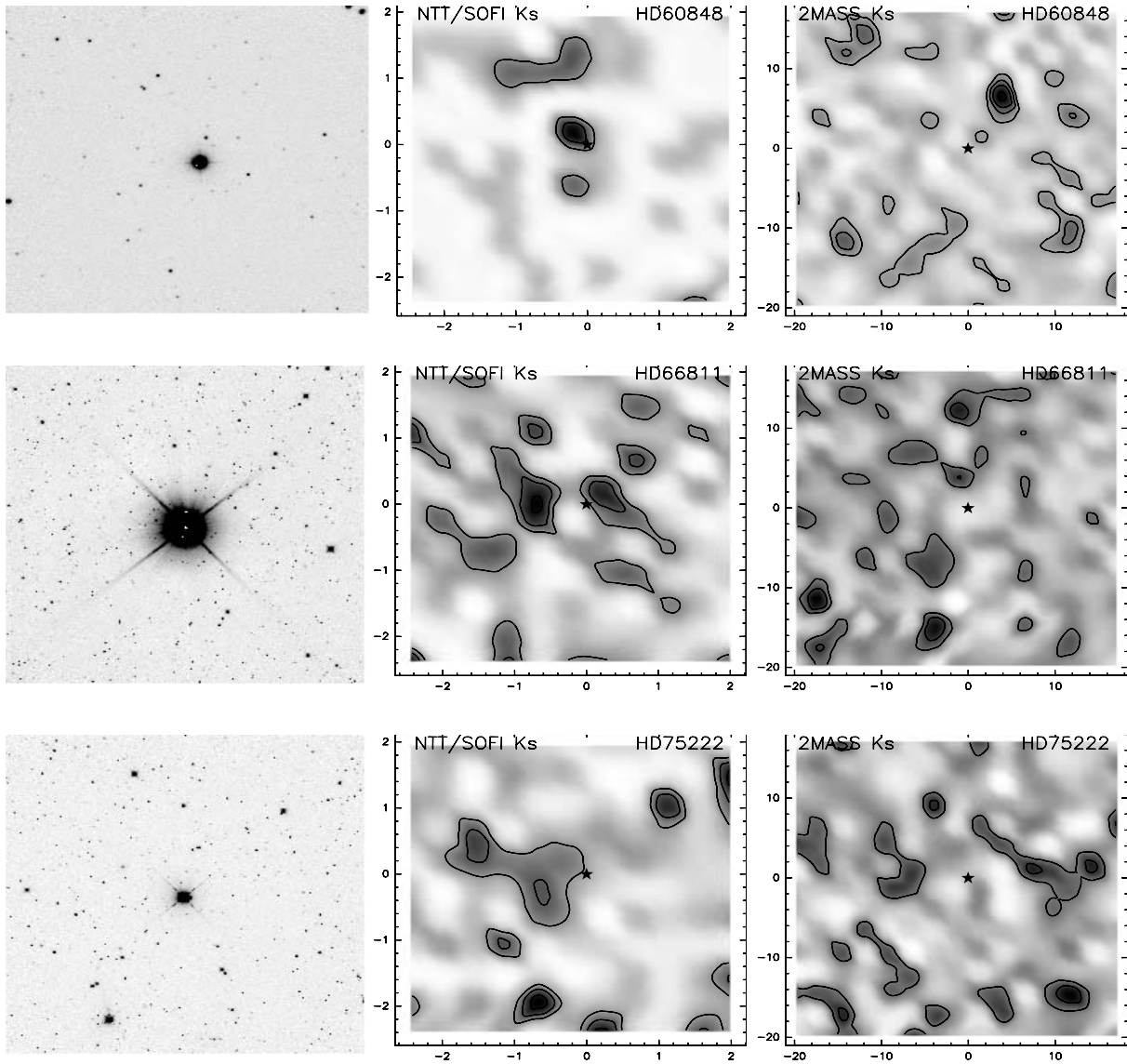


**Fig. 6.** As in Fig. 3 for stars HD 60848, HD 66811, and HD 75222.

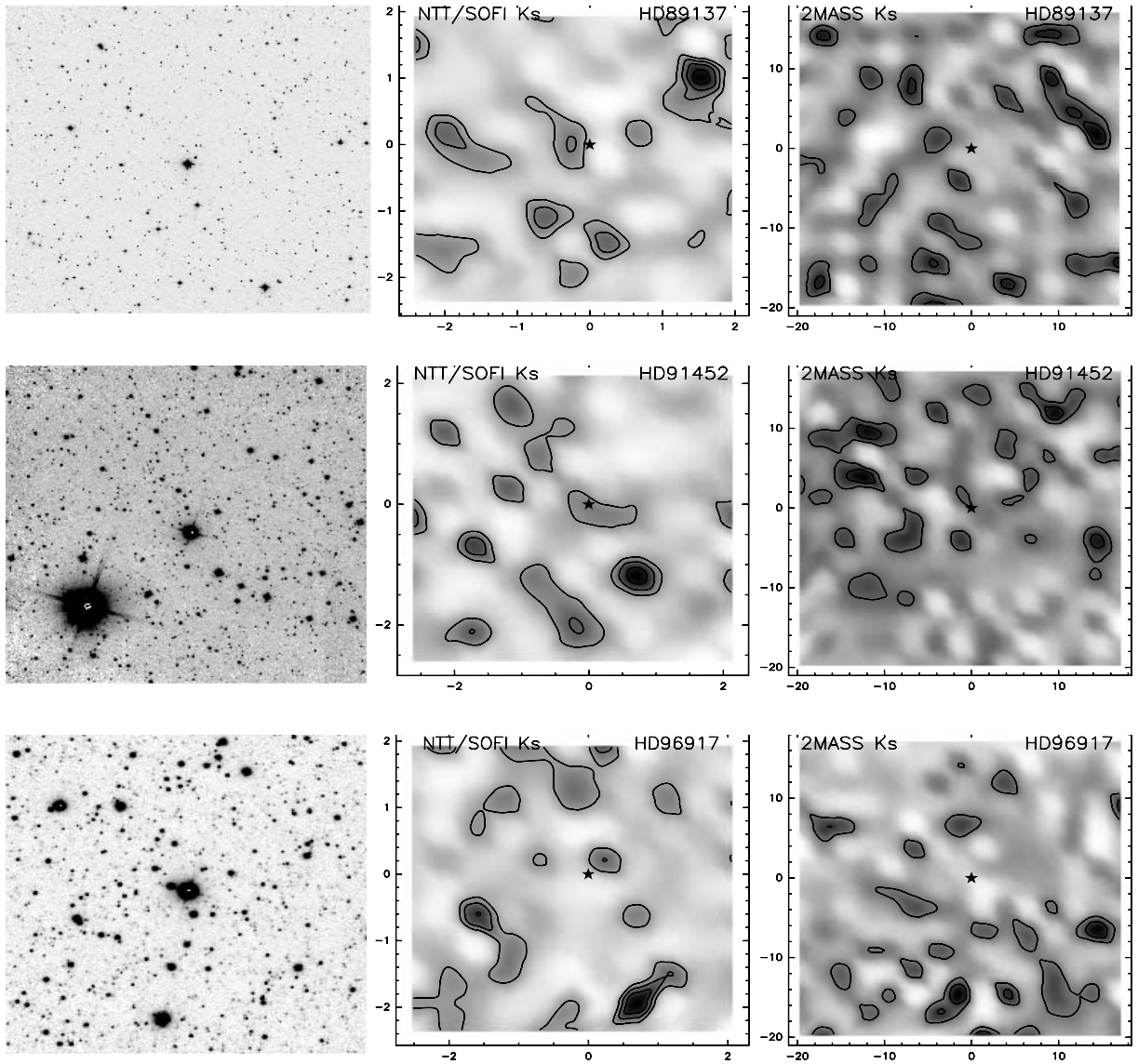


**Fig. 7.** As in Fig. 3 for stars HD 89137, HD 91452, and HD 96917.

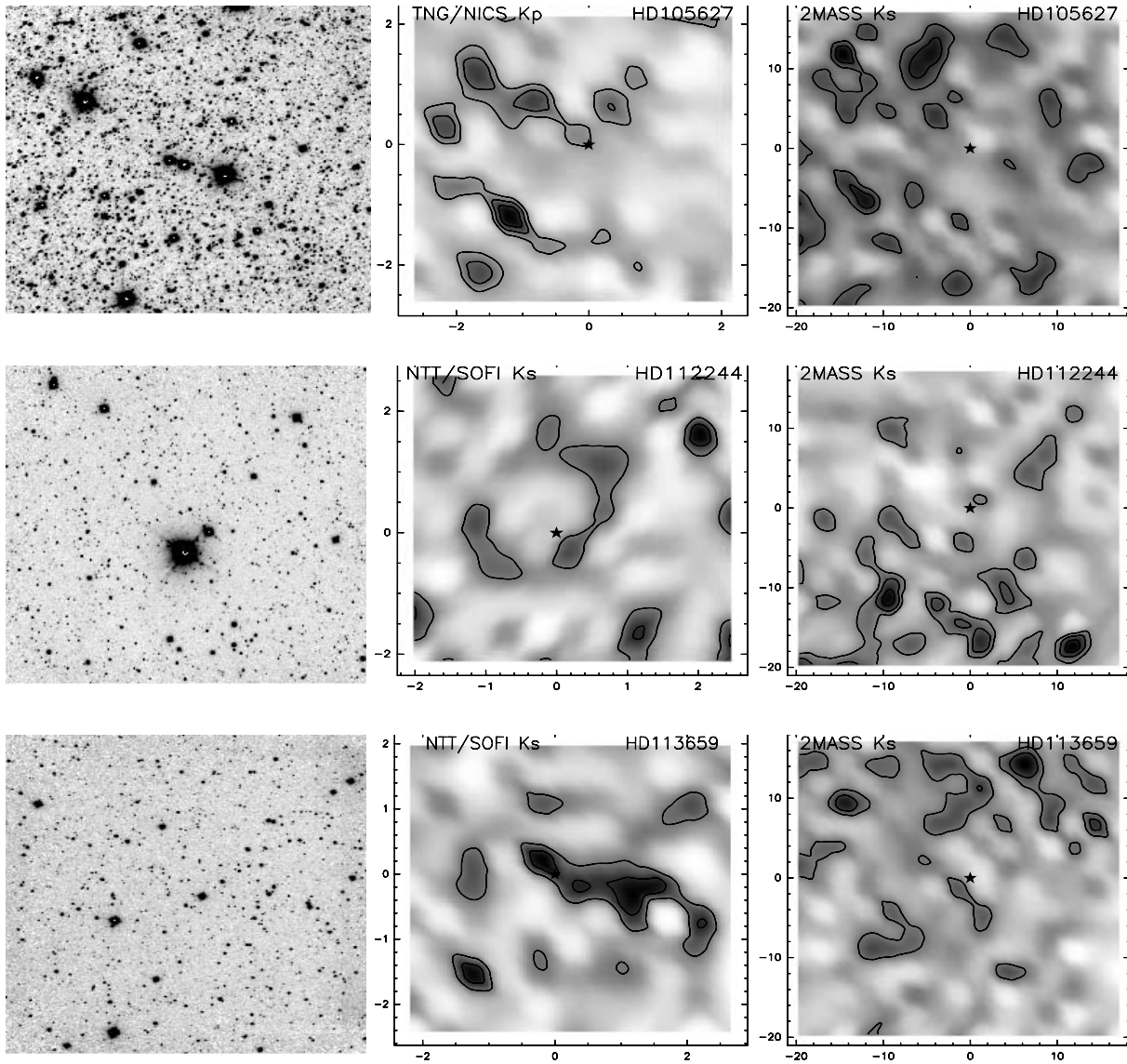


**Fig. 8.** As in Fig. 3 for stars HD 105627, HD 112244, and HD 113659.

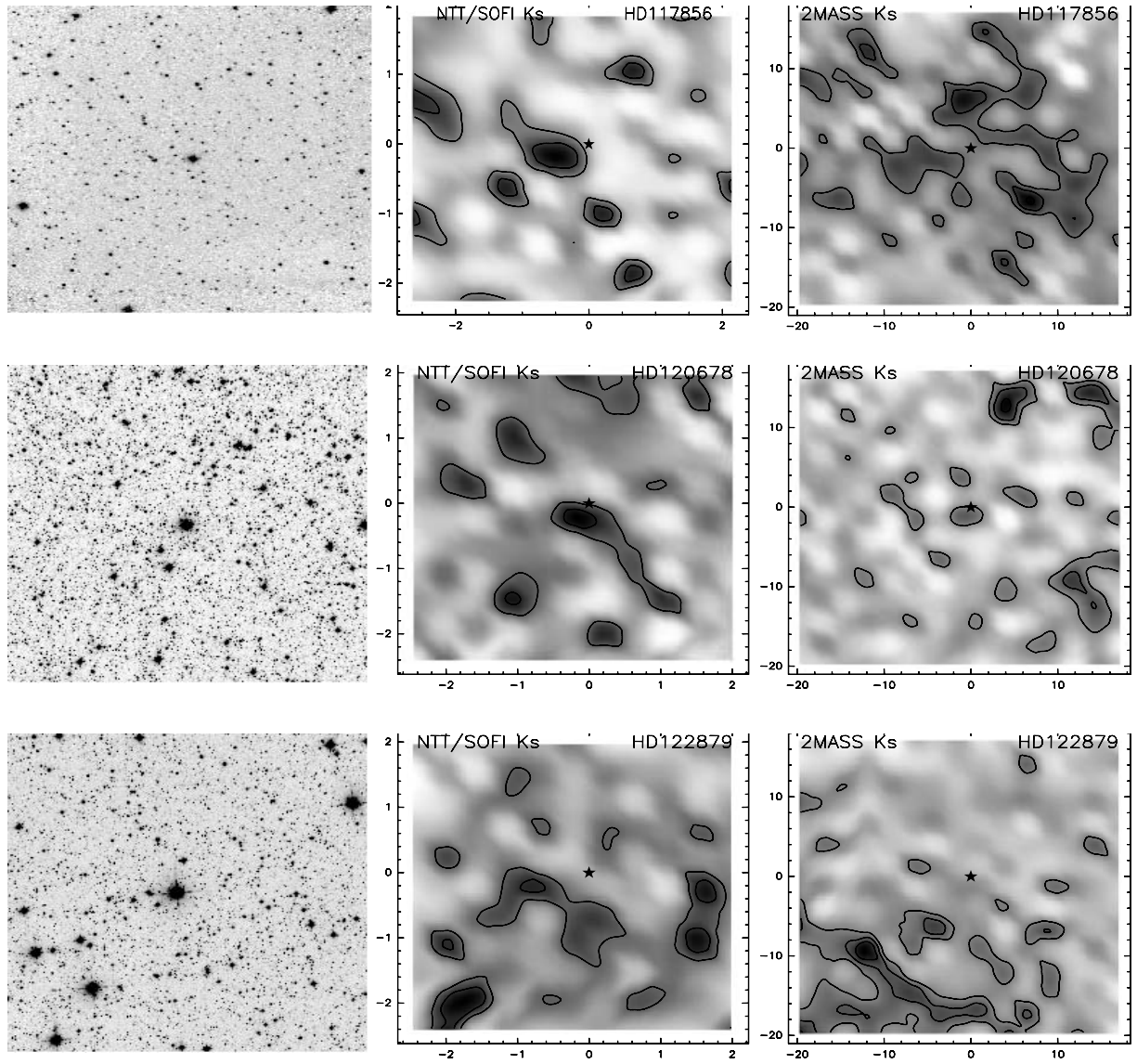


**Fig. 9.** As in Fig. 3 for stars HD 117856, HD 120678, and HD 122879.

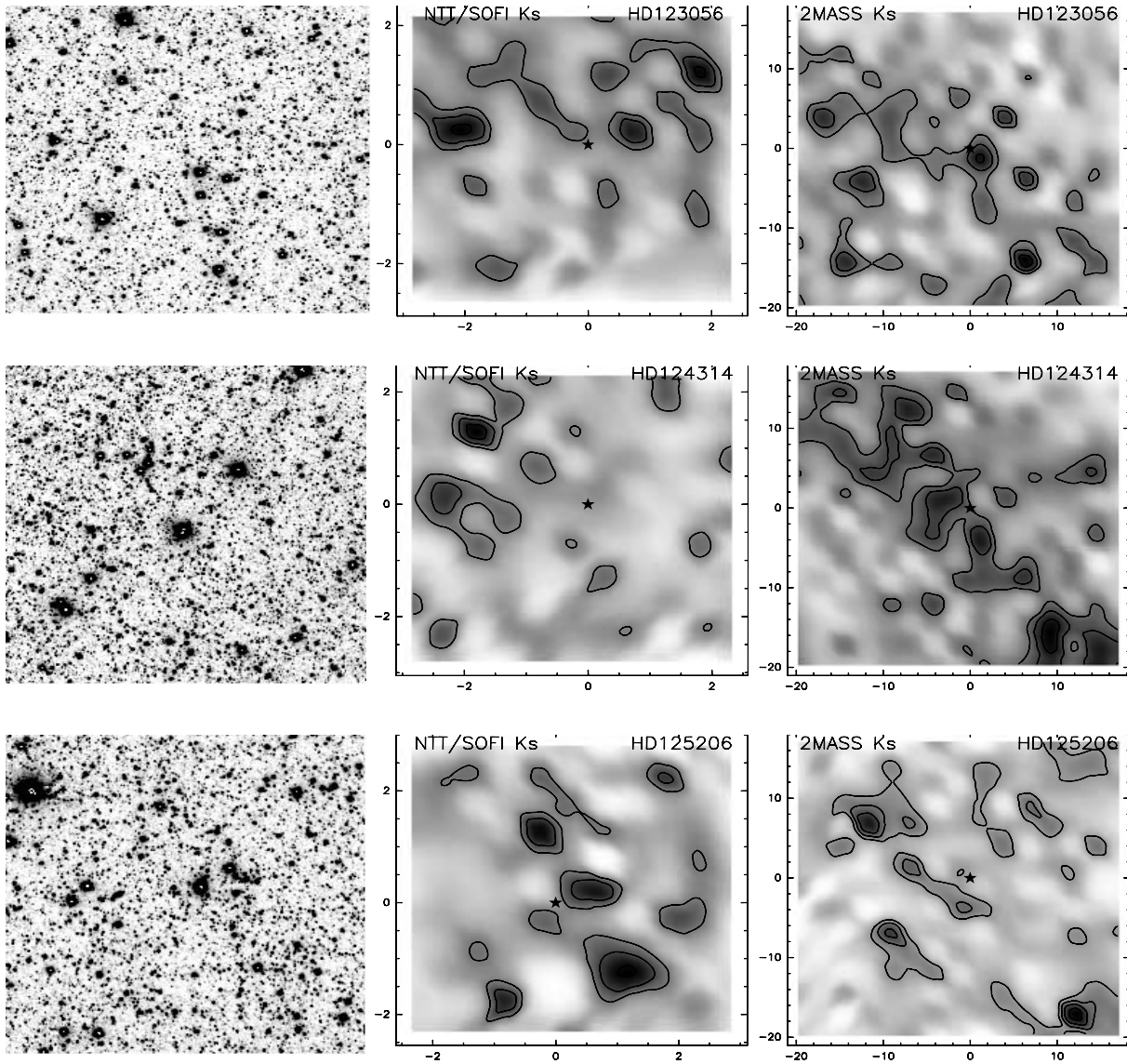


**Fig. 10.** As in Fig. 3 for stars HD 123056, HD 124314, and HD 125206.

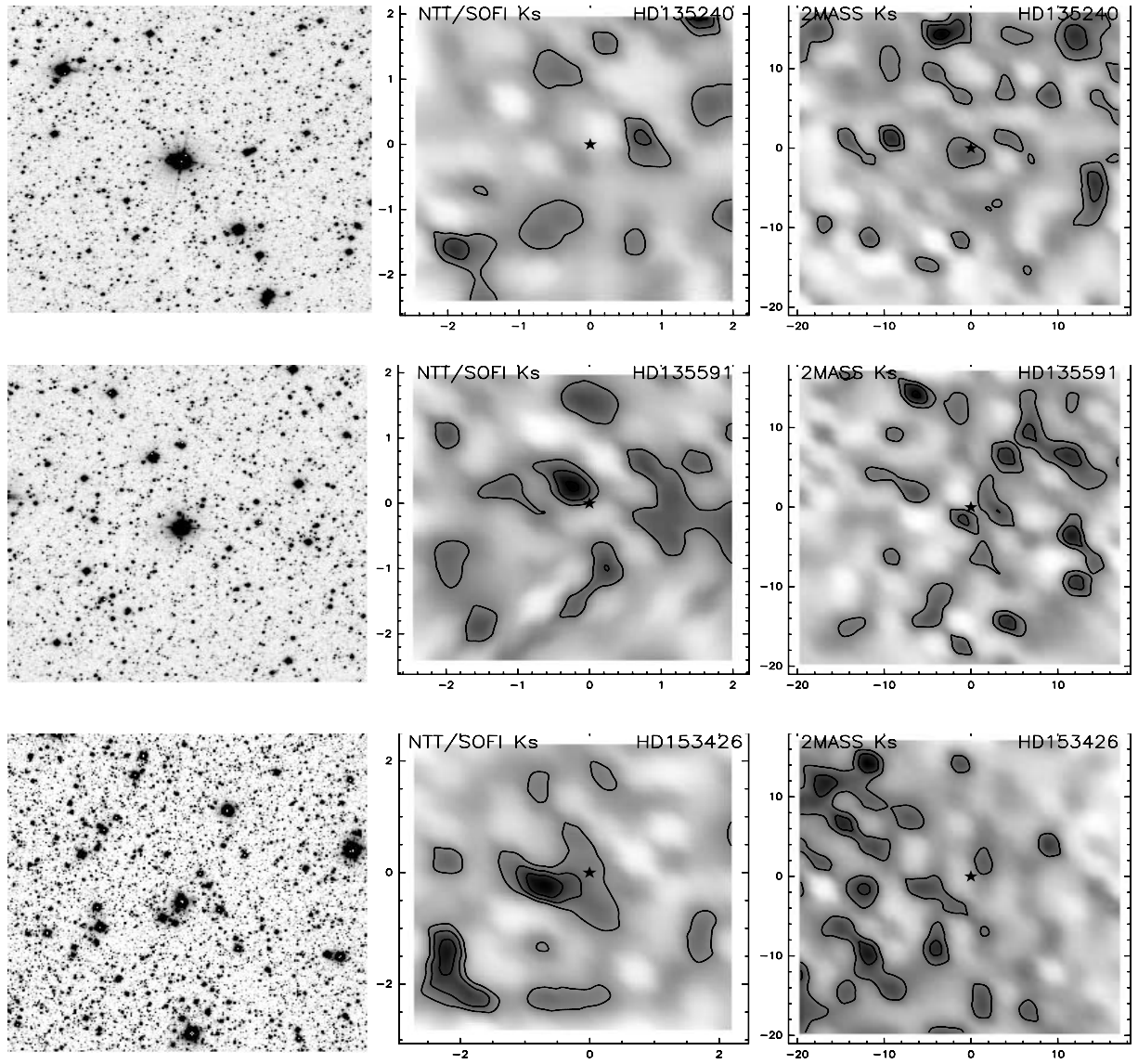


**Fig. 11.** As in Fig. 3 for stars HD 135240, HD 135591, and HD 153426.

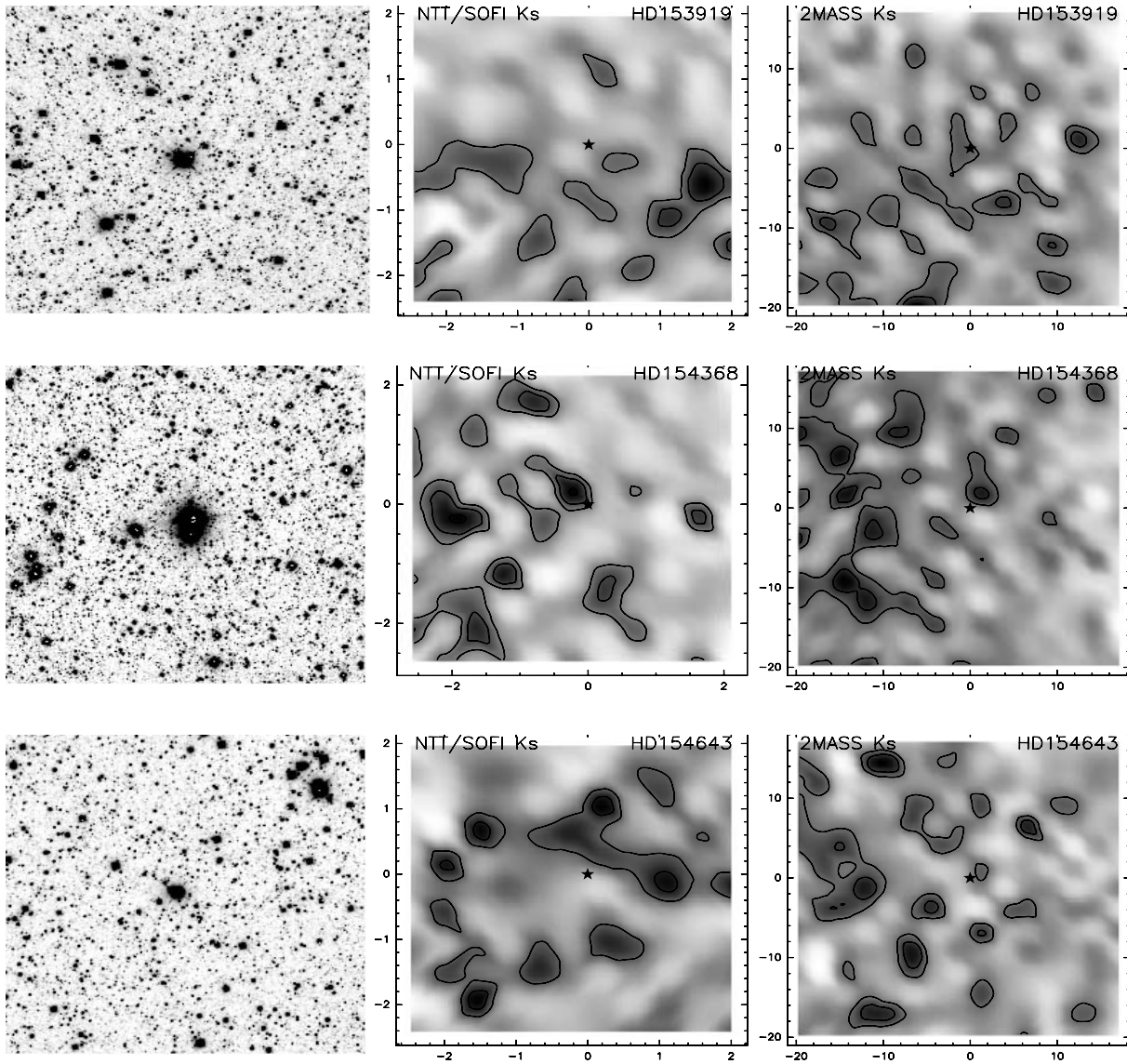


**Fig. 12.** As in Fig. 3 for stars HD 153919, HD 154368, and HD 154643.

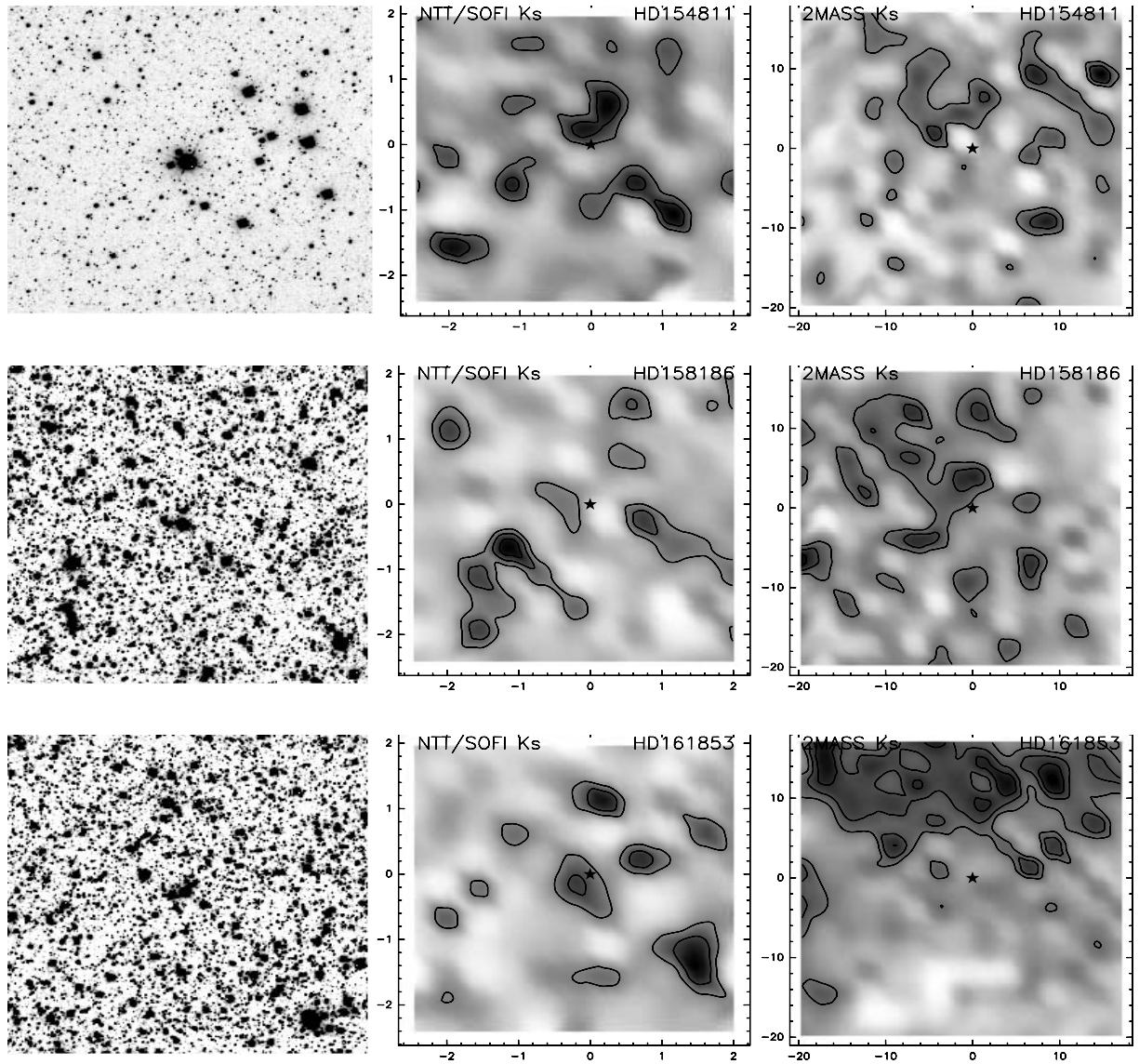


**Fig. 13.** As in Fig. 3 for stars HD 154811, HD 158186, and HD 161853.

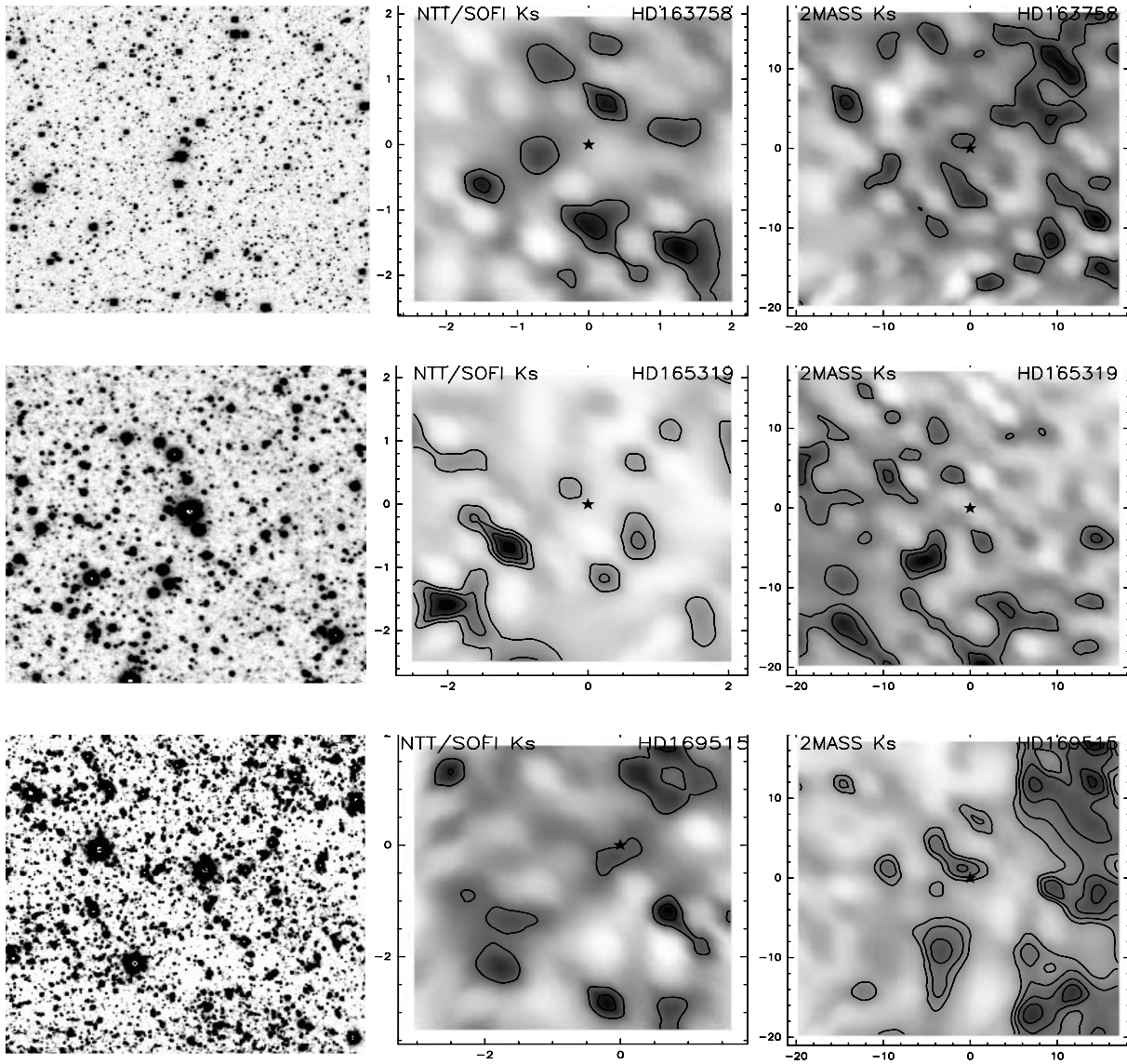


**Fig. 14.** As in Fig. 3 for stars HD 163758, HD 165319, and HD 169515.

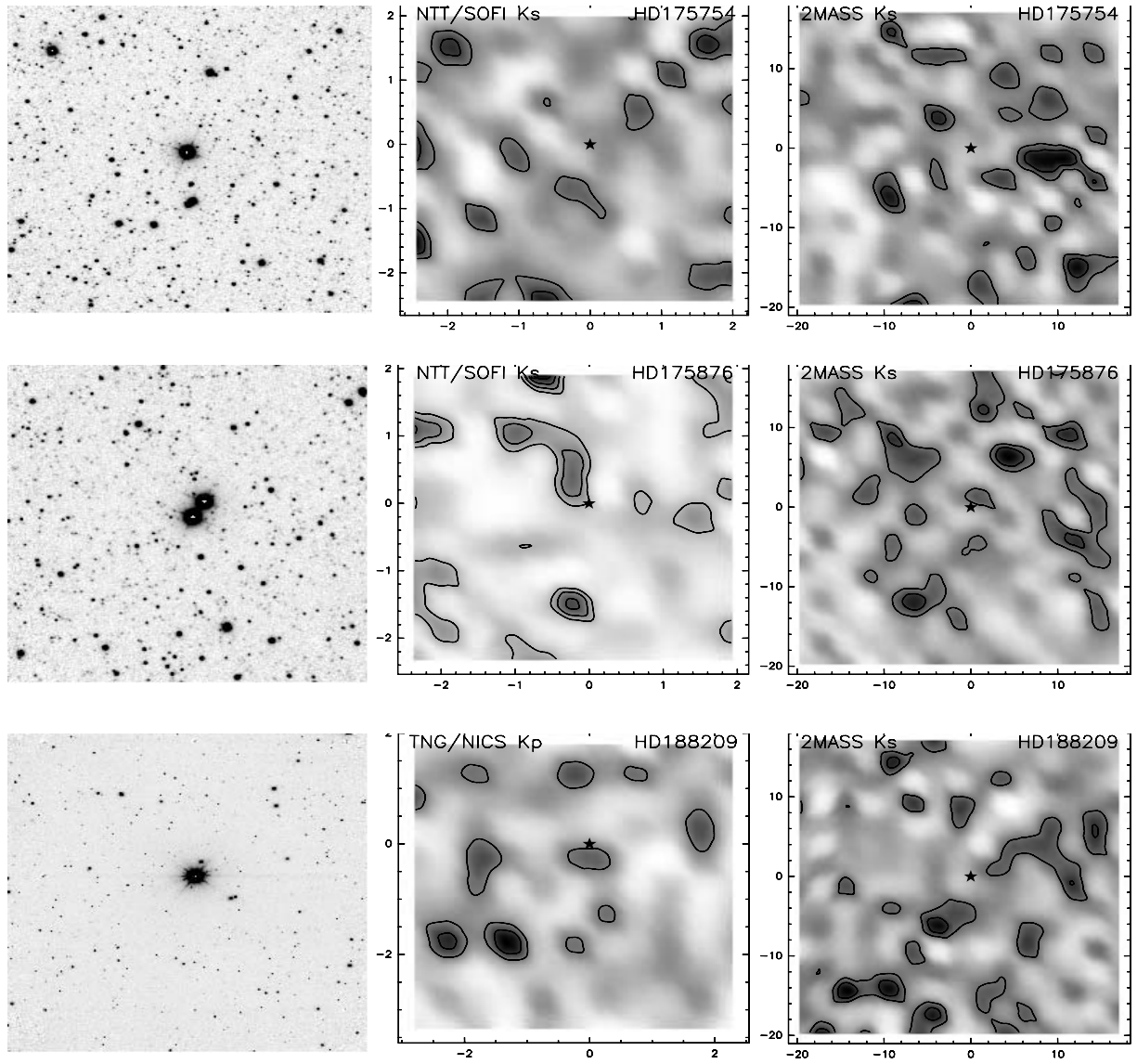


**Fig. 15.** As in Fig. 3 for stars HD 175754, HD 175876, and HD 188209.

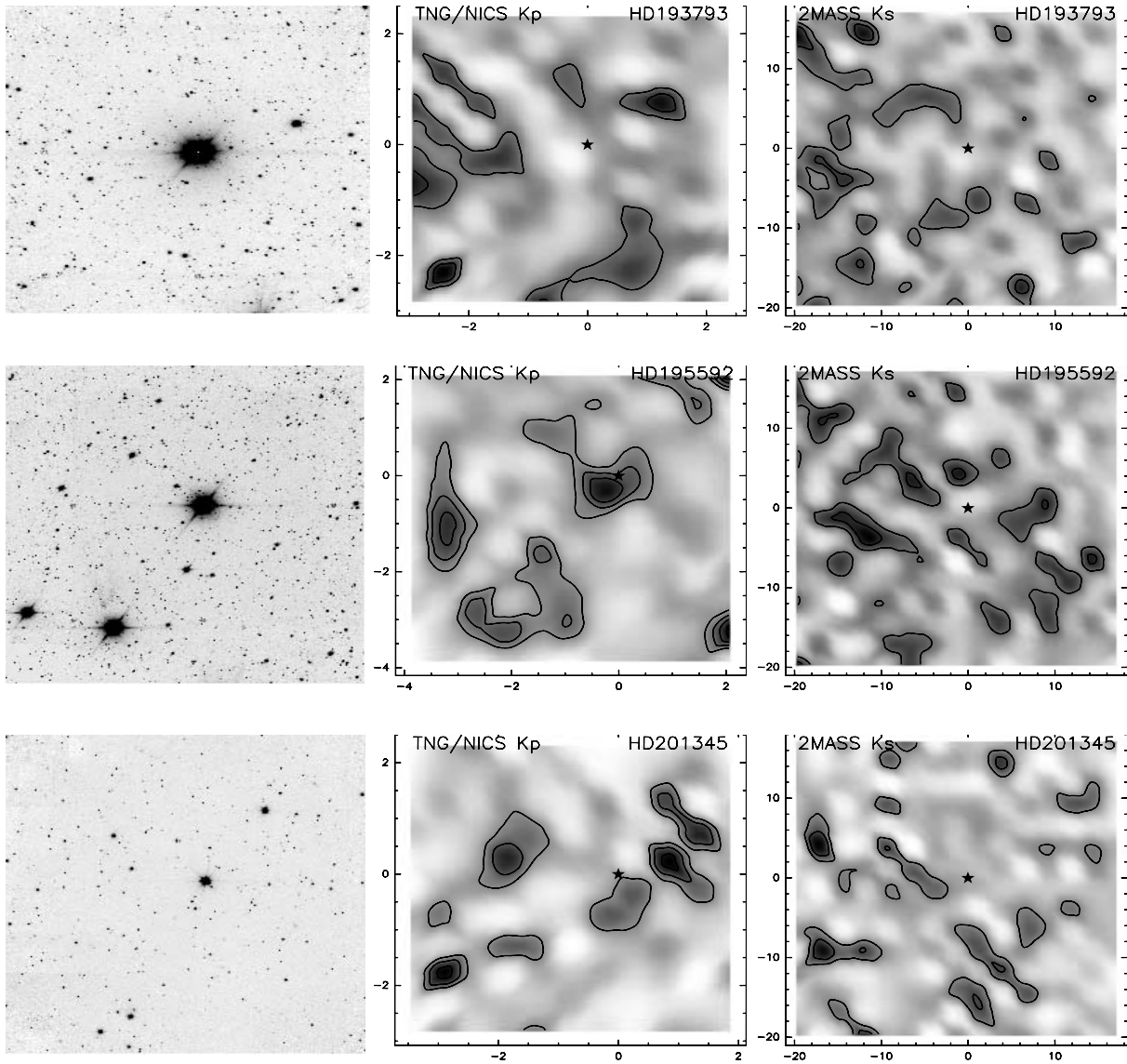


**Fig. 16.** As in Fig. 3 for stars HD 193793, HD 195592, and HD 201345.

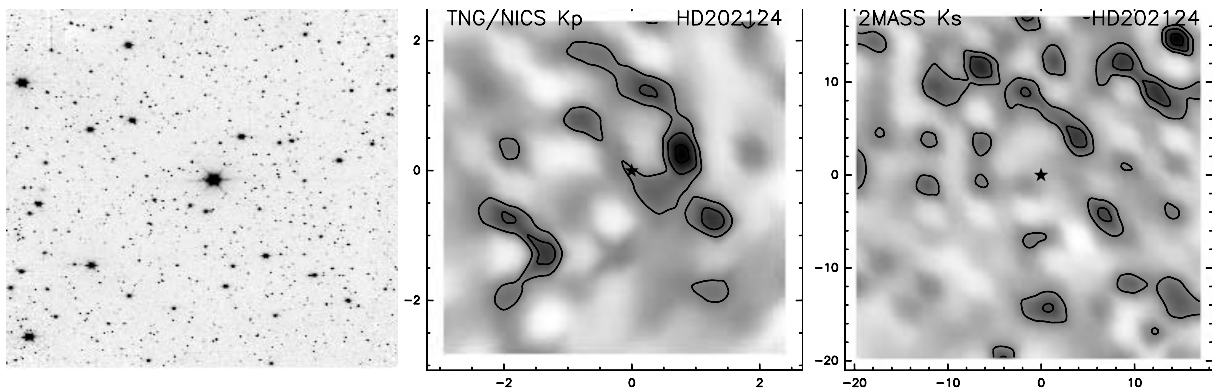


**Fig. 17.** As in Fig. 3 for star HD 202124.